Motion Detection, Object Classification and Tracking for Visual Surveillance Application

Deepak Kumar Panda

Department of Electronics and Communication Engineering
National Institute of Technology Rourkela
Rourkela-769 008, Odisha, India

Motion Detection, Object Classification and Tracking for Visual Surveillance Application

Thesis submitted in partial fulfillment

of the requirements for the degree of

Master of Technology

in

Communication and Signal Processing

by

Deepak Kumar Panda

(Roll: 210EC4316)

under the guidance of

Prof. Sukadev Meher

Department of Electronics and Communiation Engineering
National Institute of Technology Rourkela
Rourkela-769 008, Odisha, India

Department of Electronics and Communication Engg.
National Institute of Technology Rourkela
Rourkela-769 008, Odisha, India.

June 6, 2012

Certificate

This is to certify that the thesis titled ***Motion Detection, Object Classification and Tracking for Visual Surveillance Application*** by ***Deepak Kumar Panda*** is a record of an original research work carried out under my supervision and guidance in partial fulfillment of the requirements for the award of the degree of Master of Technology degree in ***Electronics and Communication Engineering*** with specialization in ***Communication and Signal Processing*** during the session 2011-2012.

Sukadev Meher
Professor

Acknowledgement

"The will of God will never take you where Grace of God will not protect you."
Thank you God for showing me the path...

I owe deep gratitude to the ones who have contributed greatly in completion of this thesis.

Foremost, I would like to express my sincere gratitude to my advisor, Prof. Sukadev Meher for providing me with a platform to work on challenging areas of Motion detection, object classification and tracking for visual surveillance application. His profound insights and attention to details have been true inspirations to my research.

I am very much indebted to Prof. Sarat Kumar Patra, Prof. Banshidhar Majhi and Prof. Kamala Kanta Mahapatra for providing insightful comments at different stages of thesis that were indeed thought provoking.

My special thanks go to Prof. Ajit Kumar Sahoo, Prof. Upendra Kumar Sahoo and Prof. Pankaj Kumar Sa for contributing towards enhancing the quality of the work in shaping this thesis.

I would like to thank all my friends and lab–mates for their encouragement and understanding. Their help can never be penned with words.

Most importantly, none of this would have been possible without the love and patience of my family. My family to whom this dissertation is dedicated to, has been a constant source of love, concern, support and strength all these years. I would like to express my heartfelt gratitude to them.

Deepak Kumar Panda

Abstract

Visual surveillance in dynamic scenes, especially for humans and vehicles, is one of the current challenging research topics in computer vision. It is a key technology to fight against terrorism, crime, public safety and for efficient management of traffic. The work involves designing of efficient visual surveillance system in complex environments. In video surveillance, detection of moving objects from a video is important for object classification, target tracking, activity recognition, and behavior understanding. Detection of moving objects in video streams is the first relevant step of information and background subtraction is a very popular approach for foreground segmentation. In this thesis, we have simulated different background subtraction methods to overcome the problem of illumination variation, background clutter, shadows, and camouflage. Object classification is done using silhouette template based classification to categorize objects into human, group of human and vehicle. Detecting and tracking of human body parts is important in understanding human activities. We have proposed two methods to overcome the problem of object tracking in varying illumination condition and background clutter. For target tracking of interested object in the consecutive video frames, we have used normalized correlation coefficient (NCC). NCC is robust to varying illumination condition. Template is updated on every frame to minimize the template drift problem and it also tries to cope with short-lived occlusion and background clutter. In order to extend the surveillance area and overcome occlusion, fusion of data from multiple cameras is employed in our project. We have tracked objects across multiple cameras with non-overlapping FOVs based on object appearances. A brightness transfer function (BTF) is determined from the cumulative histograms of the images. Matching of the object is done, with the help of Bhattacharya distance.

Contents

List of Figures

List of Tables

Chapter 1

Introduction

Visual surveillance is an active research topic in computer vision that tries to detect, recognize and track objects over a sequence of images and it also makes an attempt to understand and describe object behavior by replacing the aging old traditional method of monitoring cameras by human operators. A computer vision system, can monitor both immediate unauthorized behavior and long term suspicious behavior, and hence alerts the human operator for deeper investigation of the event. The video surveillance system can be manual, semi-automatic, or fully-automatic depending on the human intervention. In manual video surveillance system, human operator responsible for monitoring does all the task while watching the visual information coming from the different cameras. Its an a tedious and arduous job of an operator to watch the multiple screen and at the same time to be vigilant from any unfortunate event. These systems are proving to be ineffective for busy large places as the number of cameras exceeds the capability of human experts. Such systems are in widespread across the world. The semi-automatic visual surveillance system takes the help of both human operator and computer vision. Tracking of object is being done by the computer vision algorithm and the job of classification, personal identification, and activity recognition is done by the human operator. These systems use lower level of video processing, but much of the task is done with the help of human operator intervention. In the fully-autonomous system there is no human intervention and the entire job is being done by the computer vision. These systems are intelligent enough to track, classify, and identify the object. In addition, it reports and detects the suspicious behavior and does the activity recognition of the object.

Visual surveillance [1] system can provide effective and efficient application ranging from security, traffic surveillance, crowd flux statistics and congestion analysis, person identification, detection of anomalous behavior, etc. Surveillance applications are as follows:

1. **Commercial and public security**: Monitoring busy large places like market, bus stand, railway station, airports, important government buildings, monuments, banks for crime prevention and detection. In all these busy places there is a large number of inflows and outflows of people in different multiple cameras take place. It is necessary for visual surveillance system to establish the correspondence of suspected person across multiple cameras and monitor its activity to prevent any mishap and also report to the nearby police station of any unclaimed/abandoned object in the place.

2. **Military security**: Surveillance in military headquarters, access control in some security sensitive places like military arms and ammunition store, patrolling of borders, important target detection in a war zone is done with surveillance systems.

3. **Traffic surveillance**: In urban environments monitoring congestion across the road, vehicle interaction, Detection of traffic rule violation [2] such as vehicle entry in no-entry zone, illegal U-turn can be done with visual surveillance systems. The camera records the entire event and then latter the culprit can be booked on this evidence. The Video surveillance system can avert serious accidents, such that precious lives can be saved. Intelligent computer vision techniques can make the traffic congestion free, by finding out the congested road, and then diverting the traffic to other roads.

4. **Crowd flux statistics and congestion analysis**: Visual surveillance system can automatically compute the number of people entering or leaving and then estimate congestion in busy public places like platforms in railway station,

airports, and then provide congestion analysis to assist in the management of people.

5. **Anomaly detection**: Video surveillance system can analyze the behavior of people and determine whether these behaviors are normal or abnormal. Suspicious behavior can be brought to the notice of the operator and can be further tracked such that any wrong doing can be avoided. visual surveillance system set in parking area could analyze abnormal behaviors indicative of theft.

1.1 Visual Surveillance Stages

In general, processing of visual surveillance includes the following stages: background modeling, motion segmentation, classification of foreground moving objects, human identification, tracking, understanding of object behaviors, and at the end images taken from multiple cameras are fused to increase the surveillance areas.

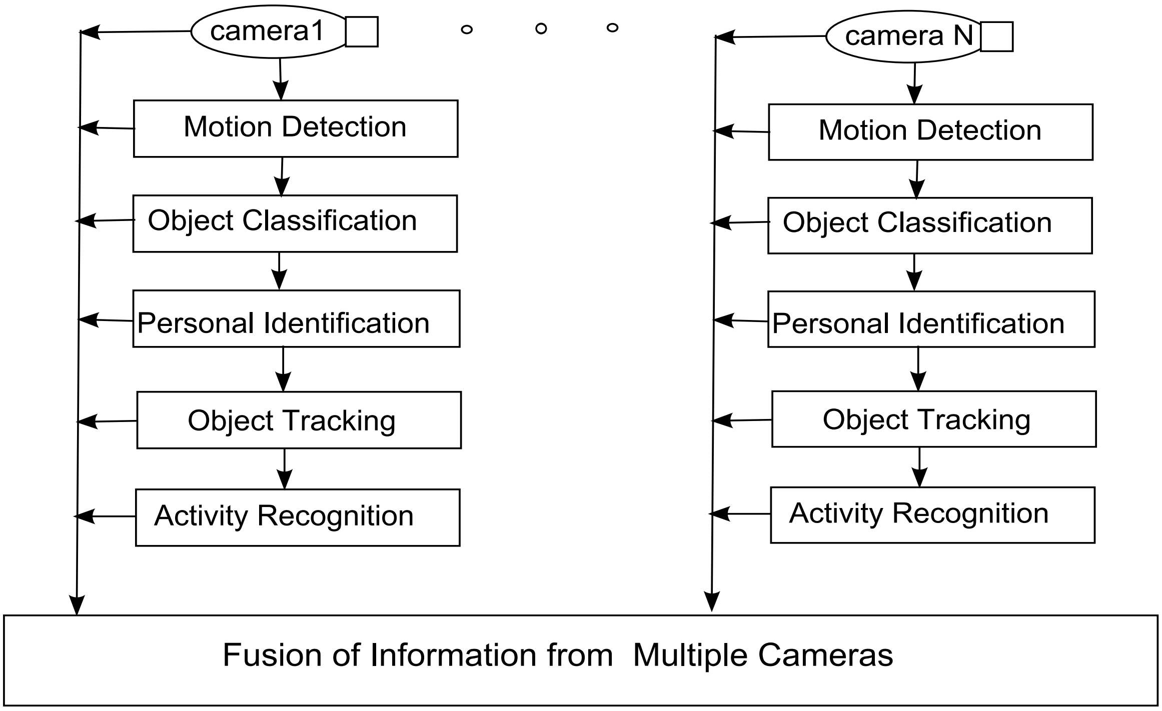

Figure 1.1: Block diagram of visual surveillance.

1.1.1 Motion Detection

First step in visual surveillance system includes motion detection. Motion detection segments the moving foreground object from the rest image. Successful segmentation of foreground object helps in the subsequent process such as object classification, personal identification, object tracking and activity recognition in the video. Motion segmentation is done mainly with background subtraction, temporal differencing, and optical flow. Out of the three methods, background subtraction is the most popular method for detecting moving regions in an image by taking the absolute difference between the current image and the reference background image. A proper threshold is judiciously selected which segments foreground from the background.

1.1.2 Object Classification

Detected moving foreground objects in an image sequence includes humans, vehicles and other moving object such as flying birds, moving clouds, animals, and abandoned object likes bags, luggages, etc. It is necessary for a video surveillance system to classify the foreground objects into the different classes and subclasses. Object classification is a standard pattern recognition problem. Classification of moving foreground object is done mainly with shape-based classification or motion-based classification. Shape-based classification uses foreground objects dispersedness, area, apparent aspect ratio, etc, as key features to classify into single human, group of human, vehicle or any other moving object such as clutter. Motion-based classification uses periodicity property of human motion for classification of humans from other moving objects.

1.1.3 Personal Identification

Once object classification is done, human needs to be identified. Personal identification of human is done through face and gait recognition [3]. Face recognition involves face detection, face tracking, face feature detection and at end recognition of face is done. Gait recognition identifies humans on their walking style. Every human has its own distinguished style of walking that makes him different from others.

1.1.4 Object Tracking

Object tracking involves tracking of moving objects from one frame to another in an video by matching objects such as points, lines or blobs. Tracking is done using the Kalman filter, the Condensation algorithm, the dynamic Bayesian network, the geodesic method, etc. Object tracking can be classified into four major categories: region based tracking, active-contour-based tracking, feature-based tracking, and model-based tracking.

1.1.5 Activity Recognition

Activity recognition is a key step in visual surveillance system that recognizes and understand behaviours of the moving foreground object. It involves the analysis and recognizes motion pattern, and it also gives description of actions and interaction. A visual surveillance system installed in a parking lot of shopping mall, will visualize and analyze the behaviour of a person coming towards the car.

1.1.6 Fusion of Information from Multiple Cameras

In order to increase the surveillance area, multiple cameras are used in visual surveillance system. Single camera object tracking can do all the above task such as object detection, classification, tracking, but the problem of occlusion can be better handle with multiple object tracking. In multiple camera object tracking, the problem of correspondence occurs and the job is to identify if the object is being tracked in some camera or the new object entered the camera FOVs. Visual surveillance using multi-camera brings problem such as camera calibration, automated camera switching and data fusion.

1.2 Overview

In this thesis, we present a real-time surveillance system for detecting moving objects, object classification, single camera object tracking and multi-camera object tracking under non-overlapping FOVs.

In Moving object detection we have simulated various background subtraction techniques available in the literature. Background subtraction involves the absolute difference between the current image and the reference updated background over a period of time. A good background subtraction should be able to overcome the problem of varying illumination condition, background clutter, shadows, camouflage, bootstrapping and at the same time motion segmentation of foreground object should be done at the real time. It's hard to get all this problem solved in one background subtraction technique. So the idea was to simulate and evaluate their performance on various video data taken in complex situations.

The object classification is a very essential step in the visual surveillance step that classifies a moving foreground object into single human, group of humans, vehicle, animals, flying birds, clutter, etc. The main target of interest in visual surveillance system application includes humans and vehicles, such that semantics from video can be used for higher level of activity analysis and task can be performed. In classification step, silhouettes of detected foreground objects from background subtraction is converted into distance signal by finding out the Euclidean distance between the centroid and the boundary of the silhouette. An object classification is done by finding out the object shape's similarity with the template stored in the database.

Single camera object tracking is a very challenging task in presence of varying illumination condition, background motion, complex object shape, partial and full object occlusion. Here in this thesis, we have proposed two methods to overcome the problem of illumination variation and background clutter such as fake motion due to the leaves of the trees, water flowing, or flag waving in the wind. Sometimes object tracking involves tracking of a single interested object and that is done using normalized correlation coefficient and updating the template.

In order to increase the surveillance area, multiple camera is being used. It's not possible for the multiple cameras to cover the entire region due to cost, finite number of camera, sensor resolution, occlusion of scene structures, and computational reasons. A brightness transfer function maps an observed intensity value in camera 1 to camera 2 is calculated. In multi-camera object tracking, the problem of correspondence occurs and the job is to locate the object from camera 1 to camera 2 using the Bhattacharya distance measure.

1.3 Motivation

Visual surveillance is the most active research topic in computer vision for humans and vehicles. Our aim is to develop an intelligent visual surveillance system by replacing the age old tradition method of monitoring by human operators. Our motivation in doing is to design a visual surveillance system for motion detection, object classification, single camera object tracking and multi-camera object tracking with non-overlapping FOVs.

1.4 Organization of the Thesis

The remaining part of the thesis is organized as follows. Chapter 2 presents a brief survey of background subtraction methods for motion segmentation. Object classification into various classes as human, vehicle, animals, birds, clutter, etc is done in Chapter 3. Tracking of Objects under varying illumination condition, background clutter and object tracking using NCC is done in Chapter 4. In Chapter 5 we have discussed object tracking in multiple cameras with non-overlapping FOV. Finally, Chapter 6 concludes the thesis with the suggestions for future research.

Chapter 2

Motion Detection

An automatic visual surveillance is used by private companies, governments and public organizations to fight against terrorism and crime, public safety in airports, bus stand, railway station, town centers and hospitals. It has also find applications in traffic surveillance for efficient management of transport networks and road safety. Visual surveillance system include task such as motion detection, object classification, personal identification, tracking, and activity recognition. Out of the task mentioned above, detection of moving object is the first important step and successful segmentation of moving foreground object from the background ensures object classification, personal identification, tracking, and activity analysis, making these later step more efficient.

Hu et al. [1] categorized motion detection into three major classes of method as frame differencing, optical flow, and background subtraction.

2.0.1 Frame differencing

Frame differencing [4] is a pixel-wise differencing between two or three consecutive frames in an image sequence to detect regions corresponding to moving object such as human and vehicles. The threshold function determine's change and it depends on the speed of object motion. It's hard to maintain the quality of segmentation, if the speed of the object changes significantly. Frame differencing is very adaptive to dynamic environments, but very often holes are developed inside moving entities.

2.0.2 Optical flow

Optical flow [5] uses flow vectors of the moving objects over time to detect moving regions in an image. It is used for motion-based segmentation and tracking applications. It is a dense field of displacement vectors which defines the translation of each pixel region. Optical flow is best suited in the presence of camera motion, but however most flow computation methods are computationally complex and are sensitive to noise.

2.0.3 Background subtraction

The background subtraction [6], [7], [8], [9], [10], and [11] is the most popular and common approach for motion detection. The idea is to subtract the current image from a reference background image, which is updated during a period of time. It works well only in the presence of stationary cameras. The subtraction leaves only non-stationary or new objects, which include entire silhouette region of an object. This approach is simple and computationally affordable for real-time systems, but are extremely sensitive to dynamic scene changes from lightning and extraneous event etc. Therefore it is highly dependent on a good background maintenance model.

Here in this chapter we have simulated different background subtraction techniques available in the literature, for motion segmentation of object. Background subtraction detects moving regions in an image by taking the difference between the current image and the reference background image captured from a static background during a period of time. The subtraction leaves only non-stationary or new objects, which include entire silhouette region of an object. The problem with background subtraction [8], [9] is to automatically update the background from the incoming video frame and it should be able to overcome the following problems:

- **Motion in the background**: Non-stationary background regions, such as branches and leaves of trees, a flag waving in the wind, or flowing water, should be identified as part of the background.

- **Illumination changes**: The background model should be able to adapt, to gradual changes in illumination over a period of time.

- **Memory**: The background module should not use much resource, in terms of computing power and memory.
- **Shadows**: Shadows cast by moving object should be identified as part of the background and not foreground.
- **Camouflage**: Moving object should be detected even if pixel characteristics are similar to those of the background.
- **Bootstrapping**: The background model should be able to maintain background even in the absence of training background (absence of foreground object).

2.1 Related Work

A large literature exists concerning moving object detection in video streams and to construct reliable background from incoming video frames. Its hard to get all the above problem solved in one background subtraction technique. So the idea was to simulate different background subtraction techniques available in the literature and evaluate their performance on various video data taken in complex situation.

2.1.1 Simple Background Subtraction

In simple background subtraction a absolute difference is taken between every current image $I_t(x, y)$ and the reference background image $B(x, y)$ to find out the motion detection mask $D(x, y)$. The reference background image is generally the first frame of a video, without containing foreground object.

$$D\left(x, y\right) = \begin{cases} 1, \text{ if } |I_t(x, y) - B(x, y)| \geq \tau \\ 0, \text{otherwise} \end{cases} \tag{2.1}$$

where τ is a threshold, which decides whether the pixel is foreground or background. If the absolute difference is greater than or equal to τ, the pixel is classified as foreground, otherwise the pixel is classified as background.

2.1.2 Running Average

Simple background subtraction cannot handle illumination variation and results in noise in the motion detection mask. The problem of noise can be overcome, if the background is made adaptive to temporal changes and updated in every frame.

$$B_t(x, y) = (1 - \alpha)B_{t-1}(x, y) + \alpha I_t(x, y) \tag{2.2}$$

where α is a learning rate. The binary motion detection mask $D(x, y)$ is calculated as follows:

$$D\left(x, y\right) = \begin{cases} 1, \text{ if } |I_t(x, y) - B(x, y)| \geq \tau \\ 0, \text{otherwise} \end{cases} \tag{2.3}$$

2.1.3 Motion Detection Based on $\Sigma - \Delta$

The sign function sgn is defined as $sgn(a) = -1$ if $a < 0$, $sgn(a) = 1$ if $a > 0$, and $sgn(a) = 0$ if $a = 0$. At each frame, $\Sigma - \Delta$ (SDE) [12] estimates the background by incrementing the value by one if it is smaller than sample, or decremented by one if it is greater than the sample. The background estimated by this method is an approximation of the median of I_t. The absolute difference between I_t and B_t, gives the difference Δ_t. The binary motion detection mask $D(x, y)$ is computed from the comparison of difference Δ_t and time variance V_t. If Δ_t is smaller than time variance V_t, it corresponds to background pixel or otherwise it is the foreground pixel. The time variance V_t of the pixels, represent their motion activity measure.

Algorithm 1: Background estimation based on $\Sigma - \Delta$

```
Result: Binary motion detection mask, $D_t(x, y)$
Initialization
$B_0(x, y) = I_0(x, y)$
$V_0(x, y) = \Delta_0(x, y)$
$N = 4$
for each frame (t) do
    for each pixel (x, y) do
        The intensity of the background decreases or increases by 1
        $B_t(x, y) = B_{t-1}(x, y) + sgn(I_t(x, y) - B_{t-1}(x, y))$
        $\Delta_t(x, y) = |I_t(x, y) - B_t(x, y)|$
        if $\Delta_t(x, y) \neq 0$ then
            time variance $V_t(x, y) = V_{t-1}(x, y) + sgn(N \times \Delta_t(x, y) - V_{t-1}(x, y))$
        Binary motion detection mask
        if $\Delta_t(x, y) < V_t(x, y)$ then
            $D(x, y) = 0$
            $else D(x, y) = 1$
```

2.1.4 Multiple Background Based on $\Sigma - \Delta$ Estimation

$\Sigma - \Delta$ estimation cannot handle complex environments and it fails to generate an accurate background when multiple objects are present or moving objects exhibits variable motion. Adaptive background generated by multiple $\Sigma - \Delta$ estimation (MSDE) [12] is based on multi-modal background model $B_t(x, y)$. MSDE can detect multiple moving object with higher degree of accuracy than SDE, but at the cost of greater computational complexity. MSDE methods computes the set of K backgrounds $\{b_t^i\}_{1 \leq i \leq K}$. A set of K variances V_t^i is also computed and Adaptive background model $B_t(x, y)$ is given by:

$$B_t(x,y) = \frac{\Sigma_{i\in[1,R]}\frac{\alpha_i(b_t^i(x,y))}{v_t^i(x,y)}}{\Sigma_{i\in[1,R]}\frac{\alpha_i}{v_t^i(x,y)}} \qquad (2.4)$$

Algorithm 2: Multiple background $\Sigma - \Delta$ estimation

```
Result: Adaptive background model, $B_t(x,y)$
Initialization
$b_t^0(x,y) = I_t(x,y)$
$V_0^i(x,y) = \Delta_0^i(x,y)$
$N = 4$, $R = 3$
$\alpha_1$, $\alpha_2$, $\alpha_3$ is set to 1, 8, and 16
for each background component (i) do
    for each frame (t) do
        for each pixel (x, y) do
            $b_t^i(x,y) = b_{t-1}^i(x,y) + sgn(b_t^{i-1}(x,y) - b_{t-1}^i(x,y))$
            $\Delta_t^i(x,y) = |I_t(x,y) - b_t^i(x,y)|$
            if $\Delta_t^i(x,y) \neq 0$ then
                $V_t^i(x,y) = V_{t-1}^i(x,y) + sgn(N \times \Delta_t^i(x,y) - V_{t-1}^i(x,y))$
for each frame (t) do
    for each pixel (x, y) do
        Adaptive background model $B_t(x,y)$ $B_t(x,y) = \frac{\Sigma_{i\in[1,R]}\frac{\alpha_i(b_t^i(x,y))}{v_t^i(x,y)}}{\Sigma_{i\in[1,R]}\frac{\alpha_i}{v_t^i(x,y)}}$
        $D(x,y) = \begin{cases} 1, \text{ if } |I_t(x,y) - B(x,y)| \geq \tau \\ 0, \text{otherwise} \end{cases}$
```

2.1.5 Advanced Motion Detection Algorithm

Advanced motion detection algorithm [13] uses rapid matching followed by accurate matching to calculate the optimum background model. The initial background model is given by the Modified Moving Average (MMA) equation computed over the K initial frames.

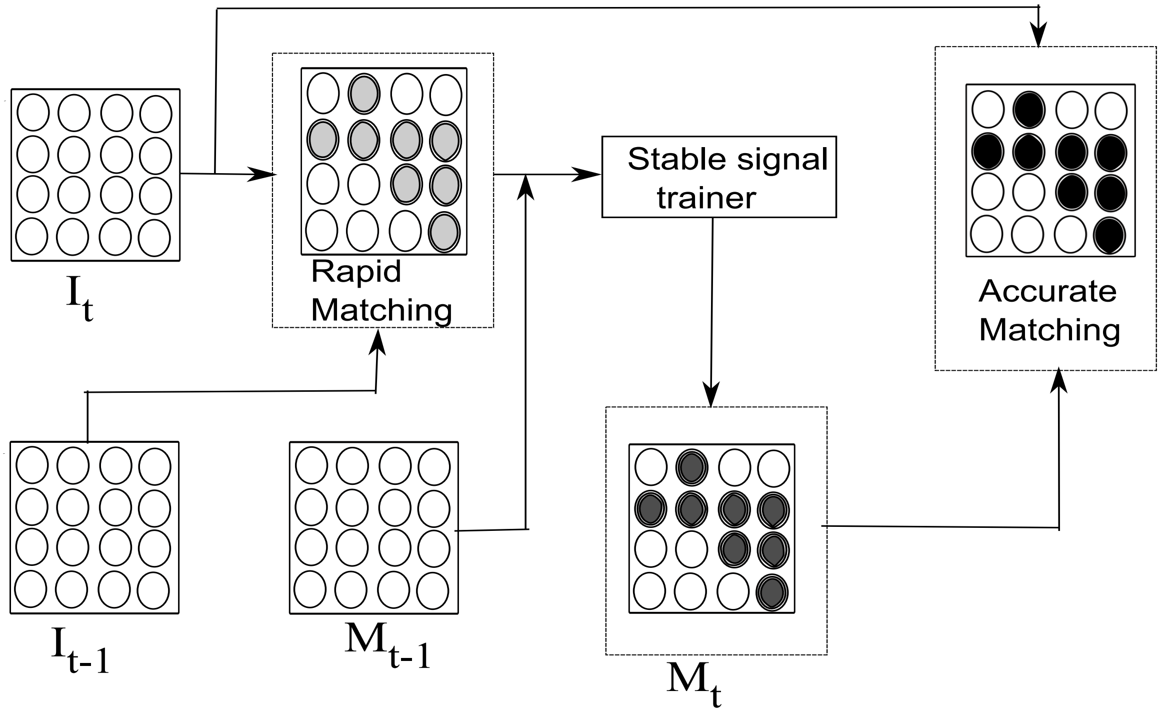

Figure 2.1: Illustration of the Optimum background Modeling Procedure.

$$B_t\left(x,y\right)=B_{t-1}\left(x,y\right)+\frac{1}{t}\left(I_t\left(x,y\right)-B_{t-1}\left(x,y\right)\right) \tag{2.5}$$

In the rapid matching the current $I_t(x, y)$ is compared to the previous $I_{t-1}(x, y)$. If the two pixel are equal, it is then sent to stable signal trainer. The stable signal trainer is expressed as follows:

$$M_t(x,y) \;=\; \begin{cases} M_{t-1}(x,y) + \; 1 \\ if \; I_t(x,y) \; > \; M_{t-1}(x,y); \\ M_{t-1}(x,y) \; - \; 1 \\ if \; I_t(x,y) \; < \; M_{t-1}(x,y); \end{cases} \tag{2.6}$$

where $M_t(x, y)$ and $M_{t-1}(x, y)$ is the current and previous set of background candidates. The initial background candidate $M_0(x, y)$ is set to $I_0(x, y)$. In the accurate matching, the current background candidate $M_t(x, y)$ is compared to $I_t(x, y)$. If the two pixels are equal, then $M_t(x, y)$ is sent to the background model $B_t(x, y)$. The current background model $B_t\left(x,y\right)$ is calculated from the moving average formula given below:

$$B_t\left(x,y\right)=B_{t-1}\left(x,y\right)+\frac{1}{\alpha}\left(I_t\left(x,y\right)-B_{t-1}\left(x,y\right)\right) \tag{2.7}$$

α is predefined parameter and is set experimentally to 8.

Once the proper background is generated from the updated background model, the absolute difference is computed between the incoming video frame $I_t(x,y)$ and updated background model $B_t(x,y)$.

$$\triangle_t(x,y)=\mid I_t(x,y)-B_t(x,y)\mid \tag{2.8}$$

The subtraction leaves only non-stationary or new objects, which include entire silhouette region of an object.

Each $w\times w$ block (i,j) within the absolute difference $\Delta_t(x,y)$ is composed of V discrete gray levels and is denoted by $\{L_0,L_1,L_2,L_3,...,L_{V-1}\}$. The block-based probability density [13], [14] function : $P_h^{(i,j)}$ is defined as

$$P_h^{(i,j)}=n_h^{(i,j)}/w^2 \tag{2.9}$$

where h represents the $\{L_0,L_1,L_2,L_3,...,L_{V-1}\}$ gray level within each $w\times w$ block (i,j), w is set at 8 and $n_h^{(i,j)}/w^2$ denotes the number of pixels corresponding to arbitrary gray-level h. The block based entropy evaluation is calculated from the given following formulae.

$$E(i,j)=-\sum_{h=0}^{L_{V-1}}P_h^{(i,j)}log2\left(P_h^{(i,j)}\right) \tag{2.10}$$

After each $w\times w$ entropy block $E(i,j)$ is calculated, the motion block A can be defined as follows:

$$A(i,j)=\begin{cases}1, & E(i,j)>T\\ 0, & otherwise\end{cases} \tag{2.11}$$

When the calculated entropy block (i,j) exceeds T, the motion block $A(i,j)$ is labeled with '1', denoting that it contains pixels of moving objects. Otherwise nonactive ones are labeled with '0'. When the block contains pixels of moving object, dilation and erosion is performed.

$$D_t(x,y) = \begin{cases} 1, \text{if } \Delta_t(x,y) > V_t(x,y) \\ 0, \text{otherwise.} \end{cases} \tag{2.12}$$

The best variance $V_t(x,y)$ is calculated from the given function

$$V_t(x,y) = N \times min\left(v_t^s(x,y), v_t^l(x,y)\right) \tag{2.13}$$

where $v_t^s(x,y)$, $v_t^l(x,y)$ represents the short-term variance and long-term variance. It is calculated through the following function for $\Delta_t(x,y)$ not equal to 0.

$$v_t^s(x,y) = \begin{cases} v_{t-1}^s(x,y) + p, \\ \text{if } N \times \Delta_t(x,y) > v_{t-1}^s(x,y); \\ v_{t-1}^s(x,y) - p, \\ \text{if } N \times \Delta_t(x,y) < v_{t-1}^s(x,y); \end{cases} \tag{2.14}$$

$$v_t^l(x,y) = \begin{cases} v_{t-1}^l(x,y) + p, \\ \text{if } N \times \Delta_t(x,y) > v_{t-1}^s(x,y); \\ v_{t-1}^l(x,y) - p, \\ \text{if } N \times \Delta_t(x,y) < v_{t-1}^s(x,y); \end{cases} \tag{2.15}$$

where v_{t-1}^s, v_{t-1}^l represents the previous short-term variance and long-term variance respectively. N is experimentally set to 2, initial v_0^s and v_0^l is set at Δ_0 and t is a multiple of α.

2.1.6 Simple Statistical Difference

Simple Statistical Difference method (SSD) computes the mean $\mu_{x,y}$ and the standard deviation $\sigma_{x,y}$ for each pixel (x,y) in the background image containing K images in the time interval $[t_0, t_{k-1}]$.

$$\mu_{xy} = \frac{1}{K}\sum_{k=0}^{K-1} I_k(x,y) \tag{2.16}$$

$$\sigma_{xy} = \left(\frac{1}{K} \sum_{k=0}^{K-1} \left(I_k(x,y) - \mu_{xy} \right)^2 \right)^{1/2} \tag{2.17}$$

For motion detection, absolute difference between the current image $I_t(x,y)$ and the mean $\mu_{x,y}$ from the background images is calculated.

$$D\left(x,y\right) = \begin{cases} 1, \text{ if } \left| I_t(x,y) - \mu_{xy} \right| \geq \lambda \sigma_{xy} \\ 0, \text{otherwise} \end{cases} \tag{2.18}$$

2.1.7 W^4 background subtraction

W^4 [10] model is a simple and effective method for segmentation of foreground objects from video frame. In the training period each pixel uses three values; minimum $m(x,y)$, maximum $n(x,y)$, and the maximum intensity difference of pixels in the consecutive frames $d(x,y)$ for modeling of the background scene. The initial background for a pixel location (x,y) is given by

$$\begin{bmatrix} m(x,y) \\ n(x,y) \\ d(x,y) \end{bmatrix} = \begin{bmatrix} \min_z \left\{ V^z(x,y) \right\} \\ \max_z \left\{ V^z(x,y) \right\} \\ \max_z \left\{ \left| V^z(x,y) \ - \ V^{z-1}(x,y) \right| \right\} \end{bmatrix}, \tag{2.19}$$
$$where \ \left| V^z(x,y) \ - \ \lambda(x,y) \right| \ < \ 2 * \sigma(x,y).$$

The background cannot remain same for a long period of time, so the initial background needs to be updated. W^4 uses pixel-based update and object-based update method to cope with illumination variation and physical deposition of object. W^4 uses change map for background updation.

A detection support map (gS) computes the number of times the pixel (x,y) is classified as background pixel.

$$gS_t(x,y) \ = \begin{cases} gS_{t-1}(x,y) + \ 1 \\ if \ pixel \ is \ background; \\ gS_{t-1}(x,y) \\ if \ pixel \ is \ foreground; \end{cases} \tag{2.20}$$

A motion support map (mS) computes the number of times the pixel (x, y) is classified as moving pixel.

$$mS_t(x,y) \ = \begin{cases} \ mS_{t-1}(x,y) + \ 1 \\ if \ M_t(x,y) \ = \ 1; \\ mS_{t-1}(x,y) \\ if \ M_t(x,y) \ = \ 0; \end{cases} \tag{2.21}$$

where

$$M_t(x,y) \ = \begin{cases} 1 \, if \ (|I_t(x,y) \ - \ I_{t+1}(x,y)| \ > \ 2*\sigma) \wedge \\ \quad (|I_{t-1}(x,y) \ - \ I_t(x,y)| \ > \ 2*\sigma) \\ 0 \quad otherwise \end{cases} \tag{2.22}$$

The new background model is given by:

$$[m(x,y), \ n(x,y), \ d(x,y)] \ = \begin{cases} \ [m^b(x,y), \ n^b(x,y), \ d^b(x,y)] \\ if \ (gS(x,y) \ > \ k*N) \ then \ pixel-based; \\ \ [m^f(x,y), \ n^f(x,y), \ d^f(x,y)] \\ if \ (gS(x,y) \ < \ k*N \ \wedge \ mS(x,y) \ < \ r*N) \\ then \ object-based; \\ \ [m^c(x,y), \ n^c(x,y), \ d^c(x,y)] \quad otherwise; \end{cases} \tag{2.23}$$

where k and r is taken to be 0.8 and 0.1 respectively. The current pixel (x, y) is classified into background and foreground by the following equation.

$$B(x,y) \ = \begin{cases} 0 \quad background & \begin{cases} ((I_t(x,y) - \ m(x,y) \ < \ kd_\mu \\ \vee \ (I_t(x,y) - \ n(x,y)) < \ kd_\mu) \end{cases} \\ 1 \quad foreground & otherwise \end{cases} \tag{2.24}$$

2.1.8 Self-Organizing Approach to Background Subtraction

Algorithm 3: SOBS (Self-Organizing Approach to Background Subtraction)

```
Result: Binary mask, $B_t(x,y)$
Initialization
model $C$ for pixel $I_0(x,y)$ and store it into $A$
$0 \leq c_2 \leq c_1 \leq 1$
$\alpha_1 = \frac{c_1}{\max(w_{i,j})}$
$\alpha_2 = \frac{c_2}{\max(w_{i,j})}$
for each frame (t) do
    $\alpha = \begin{cases} \alpha_1 - t\frac{\alpha_1 - \alpha_2}{K} & if\ 0 \leq t \leq K \\ \alpha_2 & if\ t > K \end{cases}$
    $\alpha_{i,j}(t) = \alpha(t) w_{i,j}$
    for each pixel (x, y) do
        find best match $c_m$ in $C$ to current sample $\mathrm{I}_t(x,y)$
        $\mathrm{d}(\mathrm{p}_i, p_j) = ||(v_i s_i cos(h_i), v_i s_i cos(h_i), v_i) -$
            $(\mathrm{v}_i s_i cos(h_i), v_i s_i cos(h_i), v_i)||_2^2$
        $d(c_m, p_t) = min_{i=1,\ldots,n^2} d(c_i, p_t) \leq \epsilon$
        $\epsilon = \begin{cases} \epsilon_1 & if\ 0 \leq t \leq K \\ \epsilon_2 & if\ t > K \end{cases}$
        if $c_m$ found then
            $B_t(x,y) = 0$
            update $A$ in the neighborhood of $c_m$
            for each pixel (i, j) do
                $A_t(i,j) = (1 - \alpha_{i,j}(i,j)) A_{t-1}(i,j) + \alpha_{i,j} p_t(x,y)$
        else
            if $\left(\gamma \leq \frac{p_t^V}{c_i^V} \leq \beta\right) \wedge \left(p_t^S - c_i^S \leq \tau_s\right) \wedge \left(p_t^H - c_i^H \leq \tau_H\right)$ then
                $B_t(x,y) = 0$
        else
            $B_t(x,y) = 1$
```

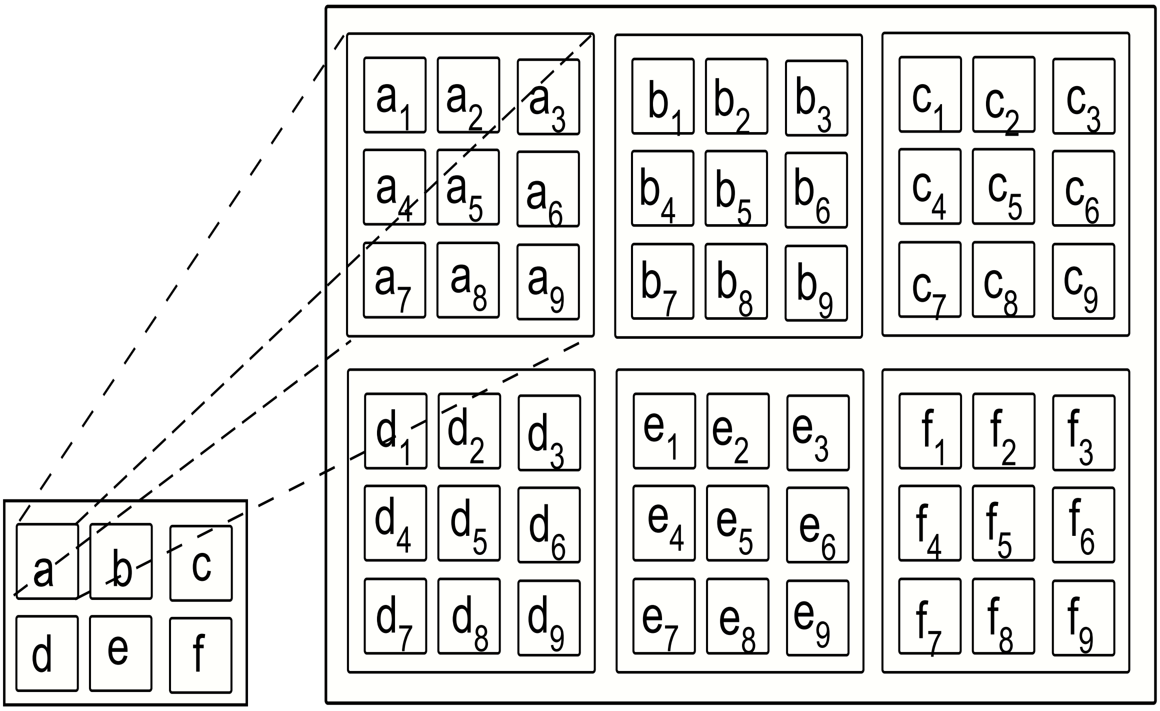
a
b
c
d
e
f
a1 a2 a3 a4 a5 a6 a7 a8 a9
b1 b2 b3 b4 b5 b6 b7 b8 b9
c1 c2 c3 c4 c5 c6 c7 c8 c9
d1 d2 d3 d4 d5 d6 d7 d8 d9
e1 e2 e3 e4 e5 e6 e7 e8 e9
f1 f2 f3 f4 f5 f6 f7 f8 f9

Figure 2.2: Neuronal map structure of self organizing background subtraction

SOBS [9] has two phases: a calibration phase and an online phase. Calibration consists in step from 1 to 19 and it involves neural network initial learning and construction of initial background. It is run over initial K number of sequence, depends on how many static frames are available in the video. Online phase involves neural network adaptation and background subtraction, steps 6 to 24 are carried in online phase and executed over $t = K + 1$ to Last frame in step 6.

2.1.9 Background Subtraction based on brightness and chromaticity distortion

Shadows cause serious problems in extracting moving objects, due to misclassification of shadows as foreground. This work exploits the lambertian hypothesis [15] to consider color as a product of irradiance and reflectance. It is based on separating the pixel value into brightness and chromaticity distortion. Background subtraction uses brightness and chromaticity distortion to classify pixel into foreground, background, shadow and highlight respectively. A pixel is modeled by a 4-tuple $\langle E_i, s_i, a_i, b_i \rangle$ where

E_i is the expected color value, s_i is the standard deviation of color value, a_i and b_i are the variation of brightness distortion and chromaticity distortion of the i^{th} pixel. The expected color value and standard deviation of i^{th} pixel is given by

$$E_i = [\mu_R(i), \mu_G(i), \mu_B(i)] \tag{2.25}$$

$$s_i = [\sigma_R(i), \sigma_G(i), \sigma_B(i)] \tag{2.26}$$

where $\mu(i)$ and $\sigma(i)$ is the arithmetic means and standard deviation of pixel i, computed over N background frames.

$$\alpha_i = \frac{\left(\frac{I_R(i)\mu_R(i)}{\sigma_R^2(i)} + \frac{I_G(i)\mu_G(i)}{\sigma_G^2(i)} + \frac{I_B(i)\mu_B(i)}{\sigma_B^2(i)}\right)}{\left(\left[\frac{\mu_R(i)}{\sigma_R(i)}\right]^2 + \left[\frac{\mu_G(i)}{\sigma_G(i)}\right]^2 + \left[\frac{\mu_B(i)}{\sigma_B(i)}\right]^2\right)} \tag{2.27}$$

$$CD_i = \sqrt{\sum_{C=R,G,B} \left(\frac{I_C(i) - \alpha_i \mu_C(i)}{\sigma_C(i)}\right)^2} \tag{2.28}$$

α_i and CD_i have different distribution for different pixels. In order to use a single threshold for every pixels, need to rescale the α_i and CD_i.

$$\hat{\alpha_i} = \frac{\alpha_i - 1}{a_i} \tag{2.29}$$

$$\widehat{CD}_i = \frac{CD_i}{b_i} \tag{2.30}$$

where $\hat{\alpha_i}$, $\widehat{CD}_i$ represents normalized brightness distortion and normalized chromaticity distortion respectively. a_i and b_i represents the variation of the brightness distortion and chromaticity distortion of the i^{th} pixel, which is given by

$$a_i = RMS(\alpha_i) = \sqrt{\frac{\sum_{i=0}^{N}(\alpha_i - 1)}{N}} \tag{2.31}$$

$$b_i = RMS(CD_i) = \sqrt{\frac{\sum_{i=0}^{N}(CD_i)^2}{N}} \tag{2.32}$$

From the above equations, a pixel in the current image is classified into one of the

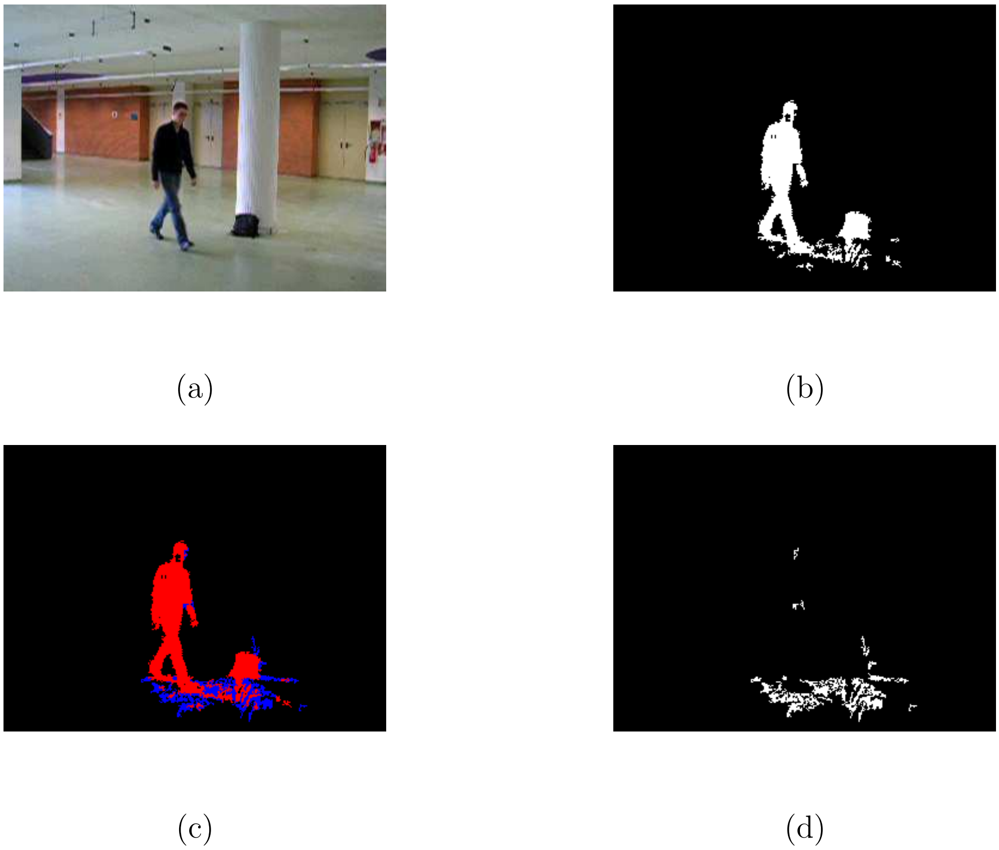

(a) (b)

(c) (d)

Figure 2.3: Results of robust background subtraction on MSA sequence (a)Original msa 336 frame , (b) foreground detection, (c) foreground is shown in red and shadow in blue, (d) shadow segmentation

four categories Foreground **F**, Background **B**, Shadow **S**, Highlight **H** by the following object mask $M(i)$ equation.

$$M(i) = \begin{cases} F: \ \widehat{CD}_i > \tau_{CD} \text{ or } \hat{\alpha}_i < \tau_{\alpha lo}, \quad \text{else} \\ B: \ \hat{\alpha}_i < \tau_{\alpha 1} \quad \text{and } \hat{\alpha}_i > \tau_{\alpha 2}, \quad \text{else} \\ S: \ \hat{\alpha}_i < 0, \quad \text{else} \\ H: \ \text{otherwise} \end{cases} \tag{2.33}$$

In this paper, τ_{CD}, $\tau_{\alpha lo}$, $\tau_{\alpha 1}$, and $\tau_{\alpha 2}$ are experimentally taken as 200000, -20, 6, and -6 respectively.

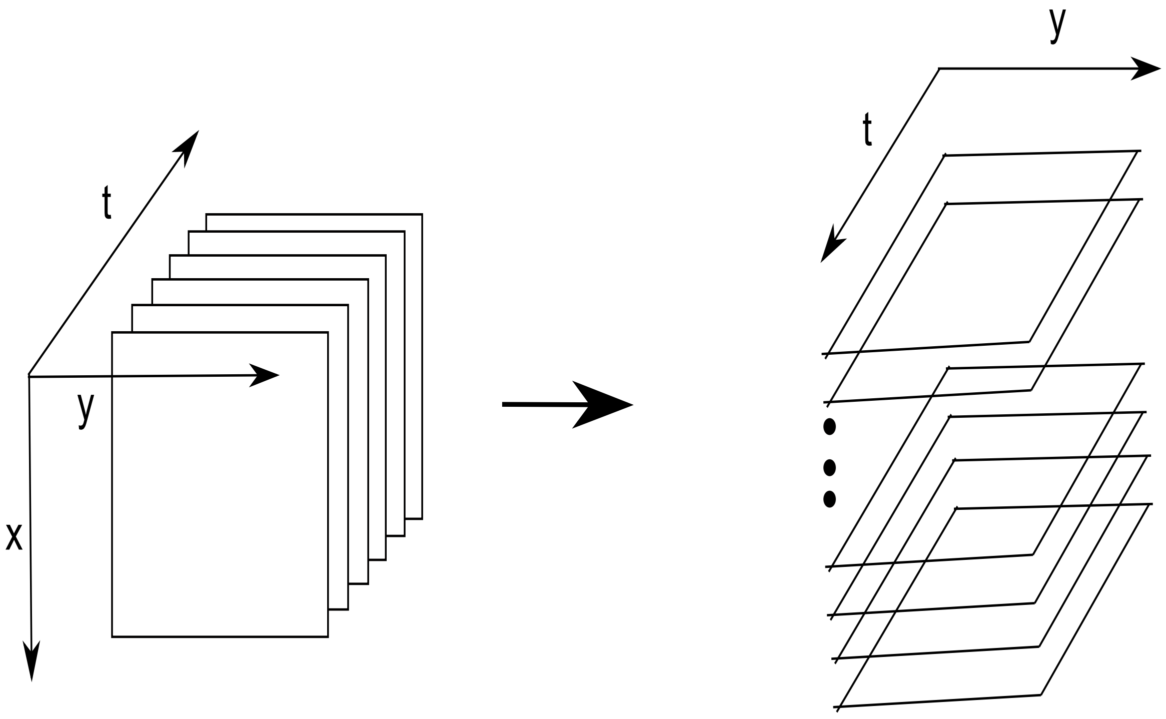

Figure 2.4: 3D spatial temporal video sliced along x-axis to get the 2D spatial-temporal image.

2.1.10 Background Subtraction using Fourier reconstruction

Let $f_t(x, y)$ be the $2D$ image of size $R \times C$ at frame t. If N frames of 2D images are stacked along 3rd dimension then a 3D spatial-temporal image of size $R \times C \times N$ can be constructed as $f(x, y, t) = f_t(x, y)$, where $x = 0, 1, 2, ..., R - 1$, $y = 0, 1, 2, ..., C - 1$ and $t = T, T - 1, ..., T - N + 1$.

Let $f_x(t, y)$ be the 2D slice of the 3D spatial-temporal image $f(x, y, t)$ along the x-axis [16], for $y = 0, 1, 2, ..., C-1$, $t = T, T-1, ..., T-N+1$, and $x = 0, 1, 2, ..., R-1$;. The 2D discrete Fourier transform (DFT) [14] of $f_x(t, y)$ is given by

$$F_x(u, v) = \frac{1}{C.N} \sum_{y=0}^{C-1} \sum_{t=0}^{N-1} f_x(y, t) \exp\left[-j2\pi \left(\frac{uy}{C} + \frac{vt}{N}\right)\right] \tag{2.34}$$

$$x = 0, 1, 2, ..., R - 1$$

where frequency variables $u = 0, 1, 2, ..., N - 1$ and $v = 0, 1, 2, ..., C - 1$.

$$F_x(u,v) = R_x(u,v) + I_x(u,v) \tag{2.35}$$

where $R_x(u,v)$ and $I_x(u,v)$ are the real and imaginary components of $F_x(u,v)$ given by:

$$R_x(u,v) = \frac{1}{C.N} \sum_{y=0}^{C-1} \sum_{t=0}^{N-1} f_x(y,t) \cos\left[2\pi\left(\frac{uy}{C} + \frac{vt}{N}\right)\right] \tag{2.36}$$

$$I_x(u,v) = -\frac{1}{C.N} \sum_{y=0}^{C-1} \sum_{t=0}^{N-1} f_x(y,t) \sin\left[2\pi\left(\frac{uy}{C} + \frac{vt}{N}\right)\right] \tag{2.37}$$

The power spectrum $P_x(u,v)$ of $F_x(u,v)$ is given by

$$P_x(u,v) = \|F_x(u,v)\|^2 = R_x^2(u,v) + I_x^2(u,v) \tag{2.38}$$

When video frames are stacked along 3D, repeated vertical line pattern appears as there are no moving objects and the background is static. The repeated vertical line patterns in the spatial domain is seen as horizontal component in the frequency domain. Static background can be removed by making the frequency components along the horizontal line and center in the Fourier spectrum to zero.

$$F_x(u,v) = 0 for \frac{N}{2} - \frac{\Delta w}{2} \leq v \leq \frac{N}{2} - \frac{\Delta w}{2} \tag{2.39}$$

In order to get back to the spatial domain, inverse discrete Fourier transform (IDFT) [14] is calculated as follow:

$$F_x(u,v) = \sum_{y=0}^{C-1} \sum_{t=0}^{N-1} f_x(y,t) \exp\left[j2\pi\left(\frac{uy}{C} + \frac{vt}{N}\right)\right] \tag{2.40}$$

$$x = 0, 1, 2, ..., R-1$$

The moving object in each video frame is obtained by reorganizing images as $f(x,y,t)$.

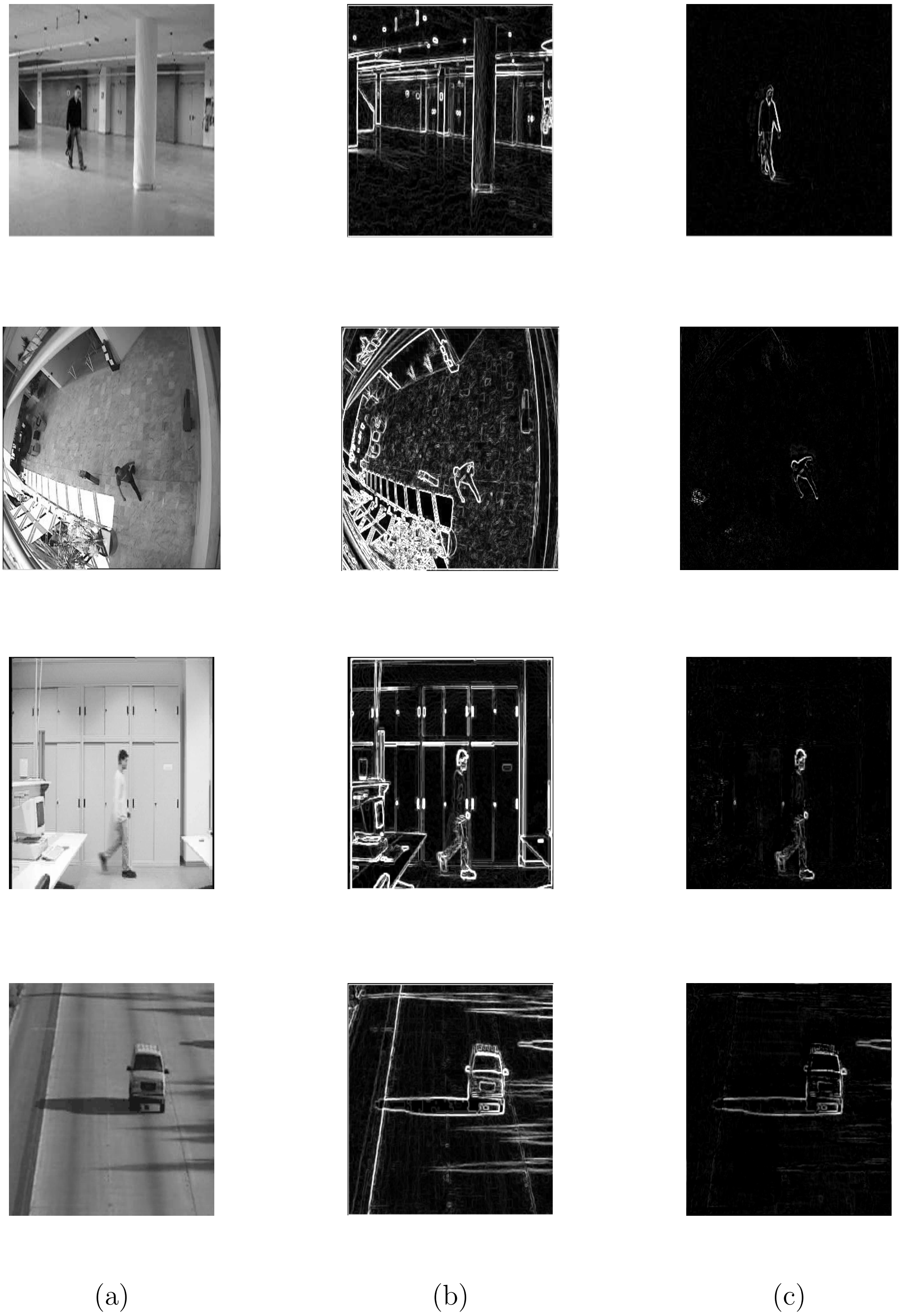

(a) (b) (c)

Figure 2.5: Motion segmentation using Fourier reconstruction (a) original image (b) gradient of image (c) foreground segmented

2.1.11 ICA-based background subtraction

ICA shows how the observed mixture signals X are obtained from mixing matrix A to mix with the latent source signal S.

$$X = AS \tag{2.41}$$

ICA solution provides solution to find out the independent signal Y, which is very close to latent source signal S, by evaluating the demixing matrix W i,e. The component of Y are mutually independent.

$$WX = Y \tag{2.42}$$

ICA is used for foreground detection [17] by finding out the demixing matrix, such that it separates the moving foreground object from the background.

$$y_t = wX_t = [w_1 w_2][x_b x_f]^T \tag{2.43}$$

where $X_t = [x_b x_f]^T$ is data matrix, x_b is the reference background image and x_t is the current image at time frame t in a video sequence. x_b and x_t are of size $[1 \times mn]$ obtained by resizing the 2-D image $f(i, j)$ of size $m \times n$ as follows:

$$\mathbf{x} = x((i-1).n + j) = f(i, j) \tag{2.44}$$

$$i = 1, 2, ..., m; j = 1, 2, ..., n$$

$w = [w_1 w_2]$ is the demixing vector matrix for separating the foreground from the background. As given in [17] the value of $w = [0.7641 - 0.6452]$ is obtained from PSO [18]. y_t is the image containing foreground object of size $[1 \times mn]$ and needs to be converted back to a 2D image by

$$I_i(u, v) = y_i(u-1).n + v) \tag{2.45}$$

$$u = 1, 2, ..., m; v = 1, 2, ..., n$$

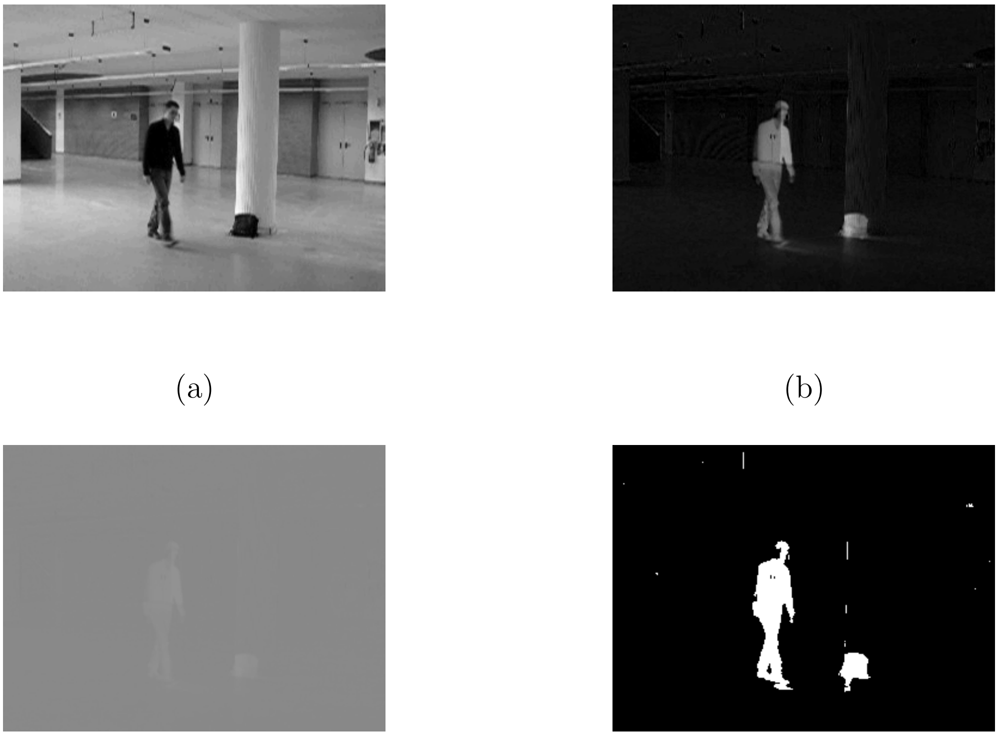

(a) (b)

(c) (d)

Figure 2.6: Background segmentation using ICA model (a) Original Image, (b) background subtraction, (c) gray image, (d) foreground detection

the 2D image containing separated foreground image $I_i(u, v)$ is converted to gray-level by

$$I_i(u, v)' = I_i(u, v).c.\sigma_b + \mu_b \tag{2.46}$$

where σ_b, μ_b are the standard deviation and mean respectively, obtained from reference background x_b. c is a constant and taken as 0.5.

The pixel is classified as foreground and background by the following equation

$$D\left(u, v\right) = \begin{cases} 0, \text{ if } I_i'(u, v) < \mu_{I' + l.\sigma_{I'}} \\ 1, \text{otherwise} \end{cases} \tag{2.47}$$

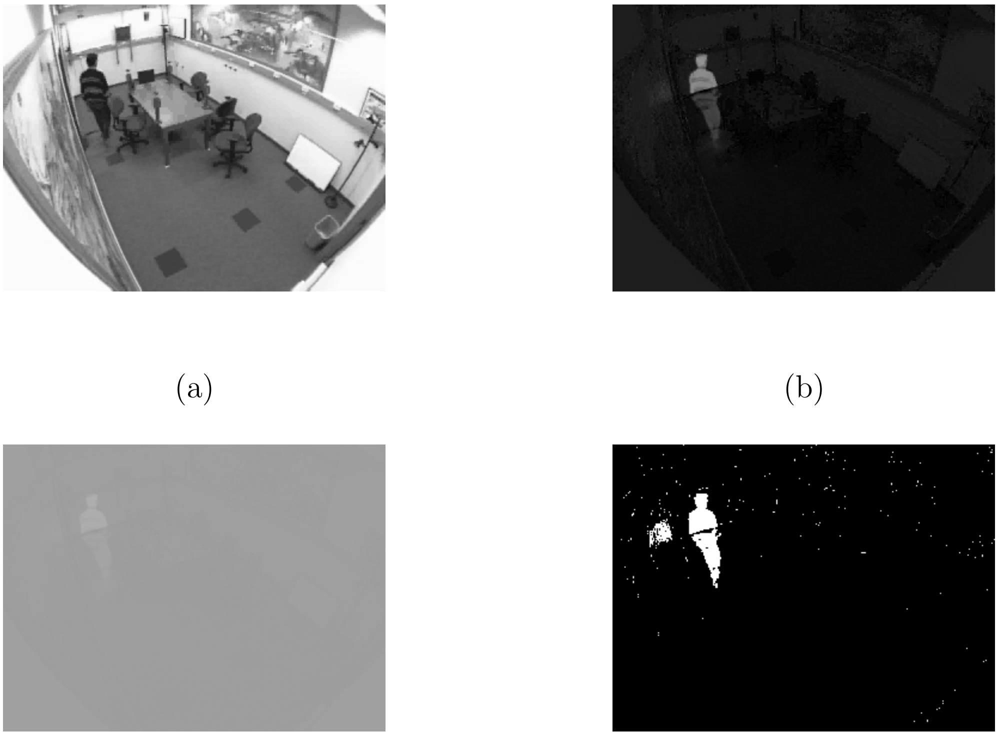

(a)

(b)

(c)

(d)

Figure 2.7: Background segmentation using ICA model (a) Original Image, (b) background subtraction, (c) gray image, (d) foreground detection

2.1.12 A Consensus-Based Background Subtraction

Wang et al. have proposed SACON [19], which keeps a cache of N background samples at each pixel such that $x_i(x, y)/i = 1, ..., N$ and $N < t$. $x_t(x, y)$ is the pixel value at time t. To overcome the problem of background subtraction, many researcher have used normalized color coordinates [7] given by

$$\begin{aligned} r &= R/(R+G+B) \\ g &= G/(R+G+B) \\ b &= B/(R+G+B) \end{aligned} \tag{2.48}$$

but this results in complete loss of intensity information, so [20], [21] have used r, g, I coordinates and $I = (R+G+B)/3$. For a pixel in shadow $(\beta \leq I_t(x, y)/I_b(x, y) \leq 1)$ and for a pixel illuminated by bright light the highlight is given by $(1 \leq I_t(x, y)/I_b(x, y) \leq \gamma)$

$$\tau_i^c(x, y, t) = \begin{cases} 1 & if\, |x_t^c - x_b^c| \leq T_r \forall c \in [r, g] \\ & \quad and\ \alpha \leq I_t(x, y)/I_b(x, y) \leq \gamma \qquad c \in [I], \\ 0 & otherwise \end{cases} \tag{2.49}$$

$$B_t(x, y) = \begin{cases} 1 & if\, \sum_{i=1}^{N} \tau_i^c(x, y, t) \geq T_n \qquad \forall c \in [r, g, I] \\ 0 & otherwise \end{cases} \tag{2.50}$$

Every background sample should be adaptive to illumination variation, adapt to new object moved or inserted in the background and it should make foreground objects which are static for a long time to be part of the background. SACON updates its background samples at both pixel level and blob level. Group of pixels below a certain size are updated at pixel level. Pixel level update is done to overcome the problem of illumination variation or small object being displaced. Pixel level update is done as follows.

$$\begin{cases} TOM_t(x,y) & = TOM_{t-1}(x,y) + 1 \\ ifB_t(x,y) = 0 & \\ TOM_t(x,y) & = 0 \\ otherwise & \end{cases} \tag{2.51}$$

Group of pixels above a certain threshold are updated at blob level as follows

$$\begin{cases} TOM_t(m^{'})_{m^{'}\in\Omega} & = TOM_{t-1}(m^{'})_{m^{'}\in\Omega} + 1 \\ if\Omega isstatic & \\ TOM_t(m^{'})_{m^{'}\in\Omega} & = 0 \\ otherwise & \end{cases} \tag{2.52}$$

2.1.13 Adaptive Background Mixture Model

A pixel at time t is modeled as mixture of K Gaussian [11] distributions. The probability of observing the current pixel value is given by

$$P(X_t) = \sum_{i=1}^{K} w_{i,t} * \eta(X_t, \mu_{i,t}, \Sigma_{i,t}) \tag{2.53}$$

where $w_{i,t}$, $\mu_{i,t}$, and $\Sigma_{i,t}$ are the estimate weight, mean value and covariance matrix of i_{th} Gaussian in the mixture at time t. $\eta(X_t, \mu_{i,t}, \Sigma_{i,t})$ is the Gaussian probability density function

$$\begin{aligned} \eta(X_t, \mu_{i,t}, \Sigma_{i,t}) &= \frac{1}{(2\pi)^{n/2} \left|\Sigma\right|^{1/2}} \exp^{-\frac{1}{2}(X_t-\mu_t)^T \Sigma^{-1}(X_t-\mu_t)} \\ \Sigma_{k,t} &= \sigma_k^2 I \end{aligned} \tag{2.54}$$

Algorithm 4: Mixture of Gaussian algorithm

```
Result: Background subtraction using Mixture of Gaussian
for each time frame $t$ do
    for for each pixel $(x, y)$ do
        for for each Gaussian component $i = 1toK$ do
            if $|X - \mu_{k,t}| \leq 2.5 * \sigma_{k,t}$ then
                $w_{k,t} = (1-\alpha)w_{k,t-1} + \alpha\,(M_{k,t})$
                $p = \alpha / w_{k,t}$
                $\mu_{k,t} = (1-p)\mu_{k,t-1} + p\,(X_t)$
                $\sigma_{k,t} = (1-p)\sigma^2_{k,t-1} + p\,(X_t - \mu_{k,t})^T\,(X_t - \mu_{k,t})$
            else
                $w_{k,t} = (1-\alpha)w_{k,t-1}$
        normalize weights $w_{k,t}$
        if none of the $k$ distributions match, create new component
        Gaussians are ordered by the value of $w/\sigma$
        first $B$ distributions are chosen as the background model
        $B = \arg min_b \left(\sum_{k=1}^{b} w_k > T\right)$
```

2.1.14 Background Subtraction in DCT Domain

A video consists of frames and each frame is divided into blocks of $[8 \times 8]$ in the spatial domain. The DCT [22] is carried out in each block such that the coefficients in the frequency domain reduces spatial redundancy. The DCT [14] is defined as

$$D(u,v) = \sum_{x=0}^{7}\sum_{y=0}^{7} F(x,y)\Gamma_{u,v}(x,y), \qquad u,v = 0,1,...,7 \tag{2.55}$$

where $F(x,y)$, $x,y = 0,1,...,7$, is the pixel value in the block, $D(u,v)$ is the corresponding DCT frequency of the block. $\Gamma_{u,v}(x,y)$ is the basis matrix for DCT.

$$\Gamma_{u,v}(x,y) = \varphi(u)\varphi(v)\cos(\pi(2x+1)u/16) \times \cos(\pi(2y+1)v/16) \qquad x,y = 0,1,...,7 \tag{2.56}$$

where $\varphi(s) = 0.5/\sqrt{2}$, if $s = 0$; $\varphi(s) = 0.5$ otherwise.

If we stack the matrix F into column wise, the resulting matrix f is $[64 \times 1]$ and if dct, of f is taken, it results in d of size $[64 \times 1]$. K is $[64 \times 64]$ kernel matrix.

$$d = Kf \tag{2.57}$$

DCT is orthogonal transform, its IDCT can be given by

$$f = K^T d \tag{2.58}$$

where K_T denotes the transpose of the matrix K.

$D_B^t = d_{t,k}^B, k = 1,2,...,L$ is the DCT coefficients at time t, where $d_{t,k}^B$ is 64-dimensional background vector for the kth pixel block at time t, L is the number of block in a frame

Running Average Algorithm in the DCT Domain

The RA algorithm in the DCT domain for calculation of background is given by

$$d_{t,k}^B =_{t,k}^B +(1-\alpha)d_{t-1,k}^B, \qquad k = 1,2,...,L \tag{2.59}$$

$d_{t,k}^B$ and $d_{t-1,k}^B$ is the background estimation of size $[64 \times 1]$ at current time frame t and previous frame $t-1$ respectively for the kth block. where $k = 1,2,...,L$ and L is the number of blocks in the image. α is the learning rate for the RA algorithm.

Median Algorithm in the DCT domain

For the median algorithm in the dct domain, each kth block's dc coefficient of DCT in the time frame $l = t, t-\Delta t, ...,$ is calculated and then out of them mid value is find out. Current background $d_{t,k}^B$ is given as follows:

Algorithm 5: Median based algorithm

```
Result: Computation and storage of median based background
for each time frame $t$ do
    for for each block $k = 1, 2, ..., L$ do
        $\mathrm{s}_{t,k} = \arg mid\,(\{DC_{l,k}, l = t, t - \Delta t, ..., \})$
        if $s_{t,k} \neq s_{t-1,k}$ then
            $d^B_{t,k} = d_{s_{t,k},k}$
    $D^t_B = d^B_{t,k}, k = 1, 2, ..., L$
```

MoG Algorithm in DCT Domain

The MoG algorithm can be modeled in the DCT domain, as 64-dimensional vector for block $k = 1, 2, ..., L$ and each block contains $i = 1, 2, ..., M$ number of component. M is taken as 3 to 5 and it depends on computations memory.

$$Pr(d_k|\lambda_k) = \sum_{i=1}^{M} w_{k,i} G_i(d_k) \tag{2.60}$$

where d_k is a 64-dimensional DCT coefficient vector for block k, $w_{k,i}$ is the weight of the block k and i denotes the number of Gaussian component. $G_i(d_k)$ is the Gaussian component density given by:

$$G_i(d_k) = 1/((2\pi)^{32}\sigma^{64}_{k,i}) \times \exp(-(d_k - \mu_{k,i})^T(d_k - \mu_{k,i})/(2\sigma^2_{k,i})) \tag{2.61}$$

where $\mu_{k,i}$ and $\sigma_{k,i}$ are the 64-dimensional mean and variance vector for the block k in the i th component.

A block is said to be matching, if it satisfies the following condition.

$$(d_k - \mu_{k,i})^T(d_k - \mu_{k,i}) < \varsigma^t_{k,i} \tag{2.62}$$

For those matching block k in the frame at time t, matching component is given by :

$$\hat{\imath} = \arg_i \min(d_k - \mu_{k,i})^T(d_k - \mu_{k,i})/\varsigma_{k,i}^{t-1} \tag{2.63}$$

where $\varsigma_{k,i}^{t-1}$ is said to be the matching threshold. and then the weight, mean and variance of the matched Gaussian component $\hat{\imath}$ is updated by the following equation

$$w_{k,\hat{\imath}}^{t} = (1-\alpha)w_{k,\hat{\imath}}^{t-1} + \alpha \tag{2.64}$$

$$\mu_{k,\hat{\imath}}^{t} = (1-\rho)\mu_{k,\hat{\imath}}^{t-1} + \rho d_k^t \tag{2.65}$$

$$\varsigma_{k,\hat{\imath}}^{t} = (1-\rho)\mu_{k,\hat{\imath}}^{t-1} + \rho(d_k - \mu_{k,i})^T(d_k - \mu_{k,i}) \tag{2.66}$$

where α is the learning rate and is usually taken to be $(0 < \alpha < 1)$ and $\rho = \alpha/w_{k,\hat{\imath}}^t$. For those un-matched components, only the weight $w_{k,\hat{\imath}}^t$ are updated as follows:

$$w_{k,\hat{\imath}}^{t} = (1-\alpha)w_{k,\hat{\imath}}^{t-1} \tag{2.67}$$

If the block doesn't satisfies the equation 2.63, the Gaussian component weight is replaced with the minimum weight, mean is replaced with the current value of the block and matching threshold is replaced with initial value. Finally the weights of all Gaussaian component are normalized.

The first S Gaussian components are chosen as background model, and S is given by

$$S = \arg_b \min(\sum_{l=i_1}^{i_b} > T) \tag{2.68}$$

where T is a threshold.

Moving Object Segmentation

In the block k at the current time frame t, moving object inside the block k is detected by the euclidean distance between the $d_{t,k}$ and $d_{t,k}^B$

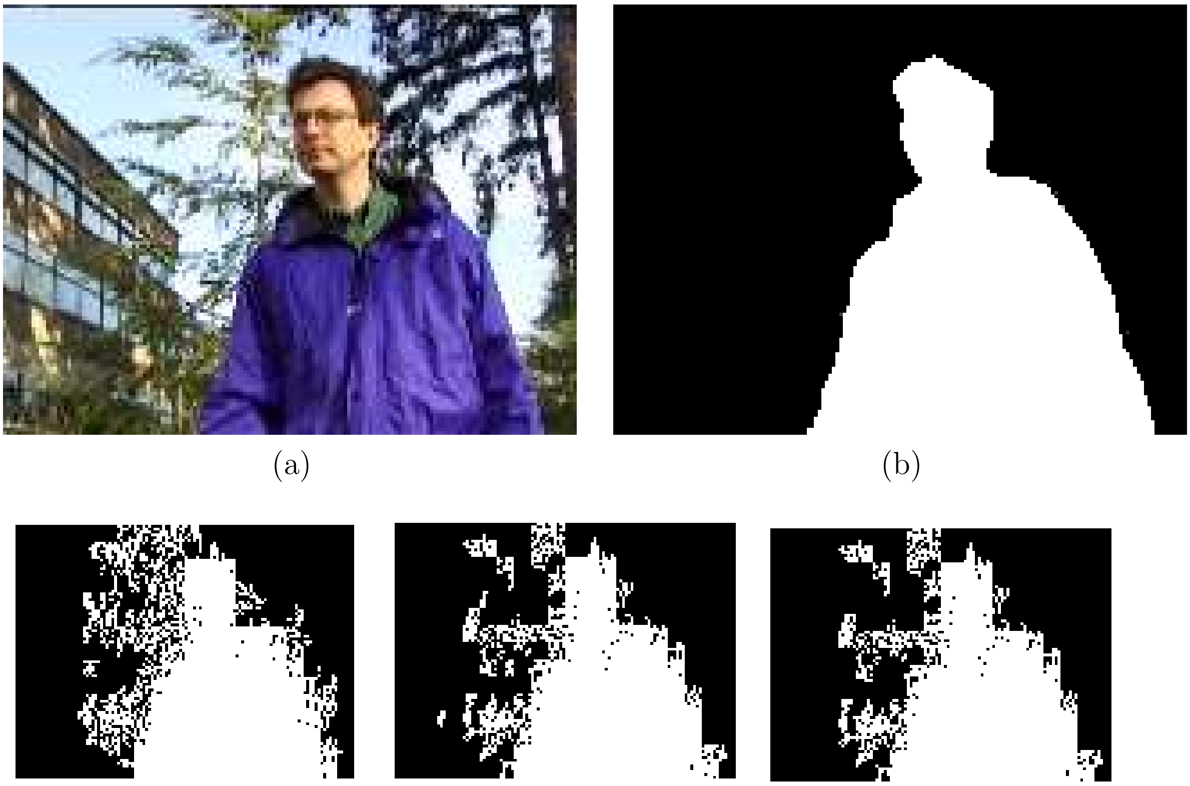

(a) (b)

(c) (d) (e)

Figure 2.8: Background subtraction using dct (a) Original Image, (b) ground-truth, (c) RA (DCT), (d) Median (DCT), (e) MoG (DCT)

$$\Omega_{t,k} = \left\| d_{t,k} - d^{B}_{t,k} \right\|_2 , k = 1, 2, ..., L \tag{2.69}$$

if $\Omega_{t,k} > \tau$, where τ is a threshold, the block k at the current time frame t is classified as foreground block. In order to classify, foreground block as foreground pixel the following relation should hold.

$$(d_Y(x,y) > T_h^{(Y)}) \vee (d_{Cb}(x,y) > T_h^{(Cb)}) \vee (d_{Cr}(x,y) > T_h^{(Cr)}) \tag{2.70}$$

or

$$(d_Y(x,y) > T_l^{(Y)}) \wedge (d_{Cb}(x,y) > T_l^{(Cb)}) \wedge (d_{Cr}(x,y) > T_l^{(Cr)}) \tag{2.71}$$

where $(d_Y(x,y)$, $(d_{Cb}(x,y)$, $(d_{Cr}(x,y)$ is the absolute difference of pixels in the spatial domain between current frame and the background . $T_l^{(c)}$, $T_h^{(c)}$, $c \in Y, Cb, Cr$ are the low and high threshold for the color coordinate c.

Waving tree [23]	**RA**	**Median**	**MoG**
Recall	0.9851	0.9841	0.9842
Precision	0.8153	0.8670	0.8718
F1	0.9928	0.9219	0.9246
Similarity	0.8054	0.8551	0.8598

Table 2.1: Pixel-based accuracy result for background subtraction in DCT

2.1.15 Background Subtraction using Codebook Model

Background subtraction using codebook (CB) [24] is an efficient algorithm that can handle illumination variation and background motion due to periodic motion in the leaves of trees.

Construction of the Initial Codebook

Let $\chi = \{x_1, x_2, ..., x_N\}$ represent training sequence for a pixel consisting of initial N background frames for an RGB vector and $C = \{c_1, c_2, ..., c_L\}$ denotes the codebook for the pixel having L codewords. Each pixel has a different length of codebook, depending on its pixel variation. Each codeword $c_i, i = 1, ..., L$ has RGB vector $v_i = (\overline{R}_i, \overline{G}_i, \overline{B}_i)$ and it also consists of 6-tuple $aux_i = \left\langle \breve{I}_i, \hat{I}_i, f_i, \lambda_i, p_i, q_i \right\rangle$. Where $\breve{I}_i, \hat{I}_i$ gives the min and max brightness, respectively, of all pixel assigned to this codeword. The frequency of occurrence of the codeword is denoted as f. λ represents the longest interval during the training of background frames that the codeword has not recurred. p, q is the first and last access that the codeword has occurred.

```
Algorithm 6: Algorithm for Codebook construction
  Result: Computation of initial codebook from N training background frames
    (I) Initialization: $L \leftarrow 0^1$, $C \leftarrow \phi$
    (II) for each $t = 1 : N$ do
        if $C = \phi$ then
            $L \leftarrow L + 1$
            $v_L \leftarrow (R, G, B)$, $aux_L \leftarrow \langle I, I, 1, t-1, t, t \rangle$.
          (i) $x_t = (R, G, B)$, $I \leftarrow \sqrt{R^2 + G^2 + B^2}$
          (ii) find the codeword $c_m$ matching to $x_t$ given by the two condition
              (a) $colordist(x_t, v_m) \leq \epsilon_1$
              (b) $brightness(I, (\check{I}_m, \hat{I}_m)) = true$
          (iii) if match then
            $v_m \leftarrow (\frac{f_m\bar{R}_m+R}{f_m+1}, \frac{f_m\bar{G}_m+G}{f_m+1}, \frac{f_m\bar{B}_m+B}{f_m+1})$
            $aux_m \leftarrow \left\langle \min\{I, \check{I}_m\}, \max\{I, \hat{I}_m\}, f_m + 1, \max\{\lambda_m, t - q_m\}, p_m, t \right\rangle$
          (iv) else
            $L \leftarrow L + 1$
            $v_L \leftarrow (R, G, B)$
            $aux_L \leftarrow \langle I, I, 1, t-1, t, t \rangle$.
    (III) for codeword $c_i, i = 1, ..., L$, do
        $\lambda_i \leftarrow \max\{\lambda_i, (N - q_i + p_i - 1)\}$.
```

Color and Brightness Distortion

pixel x_t is said to be matching the codeword c_m in $C = \{c_i | 1 \leq i \leq L$ if it satisfies the following equations.

$$colordist(x_t, v_m) \leq \epsilon_1 \tag{2.72}$$

$$brightness(I, (\breve{I}_m, \hat{I}_m)) = true \tag{2.73}$$

Color Distortion

Let $x_t = (R, G, B)$ be the input pixel and the codeword be c_i where $v_i = (\bar{R}_i, \bar{G}_i, \bar{B}_i)$

$$\left\| x_t^2 \right\| = R^2 + G^2 + B^2 \tag{2.74}$$

$$\left\| v_i^2 \right\| = \bar{R}_i^2 + \bar{G}_i^2 + \bar{B}_i^2 \tag{2.75}$$

$$\langle x_t, v_i \rangle^2 = (\bar{R}_i R + \bar{G}_i G + \bar{B}_i B)^2 \tag{2.76}$$

The color distortion δ can be computed by the following equations.

$$p^2 = \|x_t\|^2 \cos^2\theta = \frac{\langle x_t, v_i \rangle^2}{\|v_i\|^2} \tag{2.77}$$

$$colordist(x_t, v_i) = \delta = \sqrt{\|x_t\|^2 - p^2}. \tag{2.78}$$

Brightness Distortion

Each codeword has a range has a range given by

$$I_{low} = \alpha\hat{I}, I_{high} = \min\left\{\beta\hat{I}, \frac{\breve{I}}{\alpha}\right\} \tag{2.79}$$

where $\alpha < 1$ and $\beta > 1$. The value of α is taken between 0.4 and 0.7 and β is between 1.1 and 1.5. The brightness distortion is calculated as follows:

$$brightness(I, \left\langle \breve{I}, \widehat{I} \right\rangle) = \begin{cases} true & if\ I_{low} \leq \|x_t\| \leq I_{high}, \\ false & otherwise. \end{cases} \tag{2.80}$$

Foreground Detection

Algorithm 7: Algorithm for Background Subtraction

```
**Result**: Computation of initial codebook from N training background frames
    (I) $x = (R, G, B), I \leftarrow \sqrt{R^2 + G^2 + B^2}$
        Refined codebook $M = \{c_m | c_m \in C \wedge \lambda_m \leq T_M = N/2\}$
    (II) for all codeword in M, find the codeword $c_m$ matching to $x$ do
            • $colordist(x, c_m) \leq \epsilon_2$
            • $brightness(I, \left\langle \breve{I}_2, \hat{I}_m \right\rangle) = true$
        if match then
            $BGS(x, y) = 0(background)$
            Update the matched codeword
            $v_m \leftarrow (\frac{f_m \bar{R_m} + R}{f_m + 1}, \frac{f_m \bar{G_m} + G}{f_m + 1}, \frac{f_m \bar{B_m} + B}{f_m + 1})$
            $aux_m \leftarrow \left\langle \min\{I, \breve{I}_m\}, \max\{I, \hat{I}_m\}, f_m + 1, \max\{\lambda_m, t - q_m\}, p_m, t \right\rangle$
        else
            $BGS(x, y) = 1(foreground)$
```

2.2 Experimental Results

For the performance of different background subtraction technique MSA sequence [25] has been used. MSA sequence consists of 528 frames of 320 × 240 spatial resolution, acquired at a frame rate of 30 fps. In this lightning conditions are good but there is a strong shadow casted by a moving object. The scene consists of a university hall, where a man comes in, leaves a bag and goes out of the scene.

2.2.1 Accuracy Metrics

For measuring accuracy, different metrics such as precision, Recall, F_1, and Similarity is calculated and tested with msa.1130, msa.1266, msa.1296, and msa.1336 sequence of MSA video.

$$Recall = \frac{t_p}{t_p + f_n} \tag{2.81}$$

$$Precision = \frac{t_p}{t_p + f_p} \tag{2.82}$$

$$Recall = \frac{2 * Recall * Precision}{Recall + Precision} \tag{2.83}$$

$$Similarity = \frac{t_p}{t_p + f_n + f_p} \tag{2.84}$$

W4 (frame) →	130	266	296	336
Recall	0.9991	0.9986	0.9988	0.9995
Precision	0.9991	0.9934	0.9939	0.9865
F1	0.9928	0.9960	0.9963	0.9930
Similarity	0.9856	0.9920	0.9927	09860

Table 2.2: Pixel-based accuracy result for W4

SOBS (frame) →	130	266	296	336
Recall	0.9979	0.9973	0.9979	0.9977
Precision	0.9989	0.9976	0.9979	0.9973
F1	0.9984	0.9974	0.9979	0.9975
Similarity	0.9967	0.9949	0.9958	0.9950

Table 2.3: Pixel-based accuracy result for SOBS

RBS (frame) →	130	266	296	336
Recall	0.9981	0.9976	0.9984	0.9984
Precision	0.9917	0.9931	0.9937	0.9888
F1	0.9949	0.9953	0.9960	0.9936
Similarity	0.9899	0.9907	0.9920	0.9872

Table 2.4: Pixel-based accuracy result for RBS

ICA (frame) →	130	266	296	336
Recall	0.9981	0.9965	0.9974	0.9975
Precision	0.9897	0.9960	0.9960	0.9971
F1	0.9938	0.9962	0.9967	0.9973
Similarity	0.9878	0.9925	0.9934	0.9947

Table 2.5: Pixel-based accuracy result for ICA

SACON (frame) →	130	266	296	336
Recall	0.9942	0.9918	0.9921	0.9911
Precision	0.9974	0.9969	0.9976	0.9963
F1	0.9958	0.9944	0.9949	0.9937
Similarity	0.9917	0.9888	0.9898	0.9874

Table 2.6: Pixel-based accuracy result for SACON

MoG (frame) →	130	266	296	336
Recall	0.9994	0.9814	0.9780	0.9917
Precision	0.9749	0.9969	0.9998	0.9605
F1	0.9870	0.9891	0.9888	0.9759
Similarity	0.9743	0.9783	0.9778	0.9529

Table 2.7: Pixel-based accuracy result for MoG

CB (frame) →	130	266	296	336
Recall	0.9978	0.9973	0.9979	0.9976
Precision	0.9988	0.9979	0.9981	0.9969
F1	0.9983	0.9976	0.9980	0.9972
Similarity	0.9967	0.9952	0.9960	0.9945

Table 2.8: Pixel-based accuracy result for CB

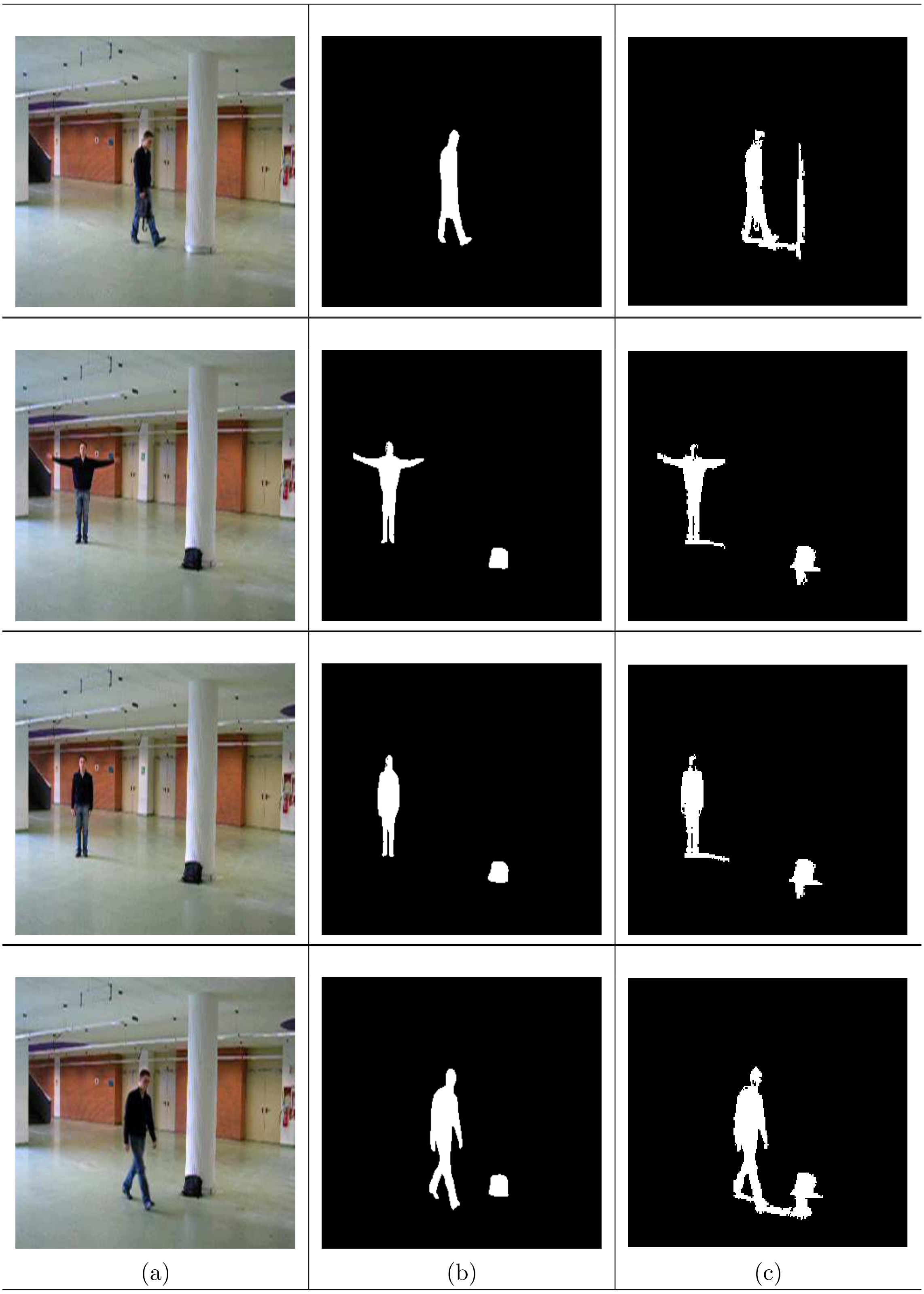

Figure 2.9: (a) MSA image (b) ground truth (c) W4 result

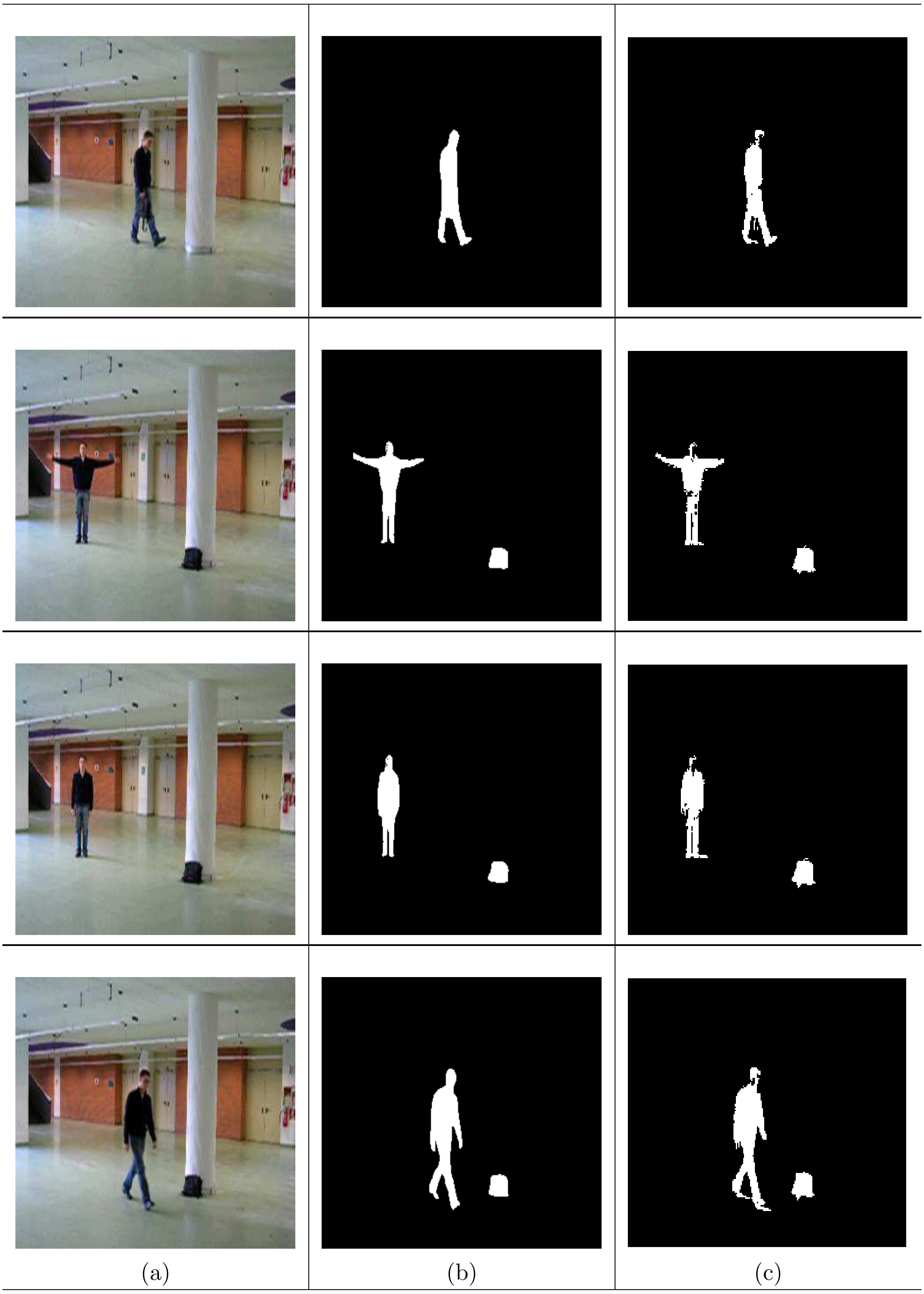

(a) (b) (c)

Figure 2.10: (a) MSA image (b) ground truth (c) SOBS result

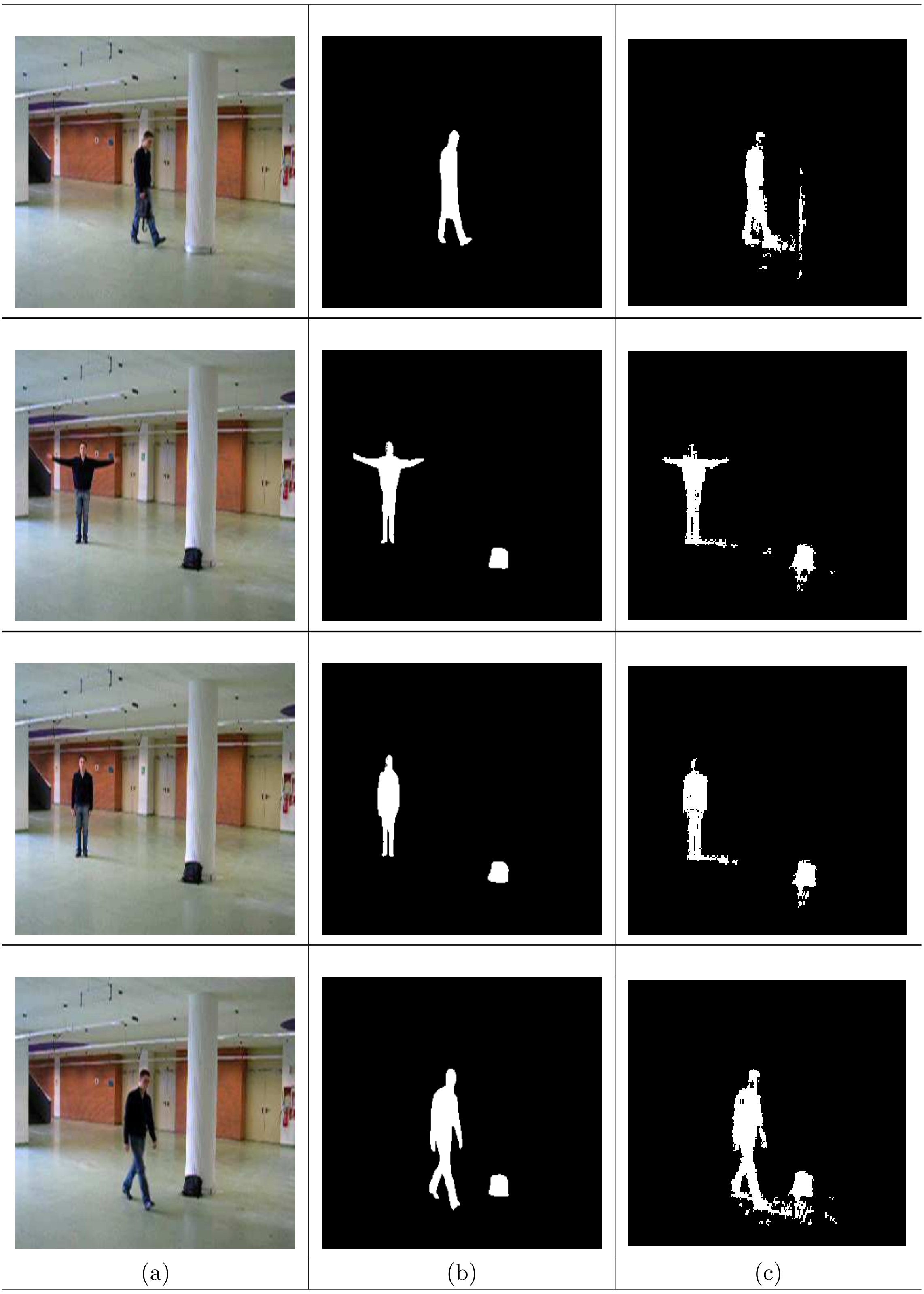

(a) (b) (c)

Figure 2.11: (a) MSA image (b) ground truth (c) Result of robust background subtraction using brightness and chromaticity distortion

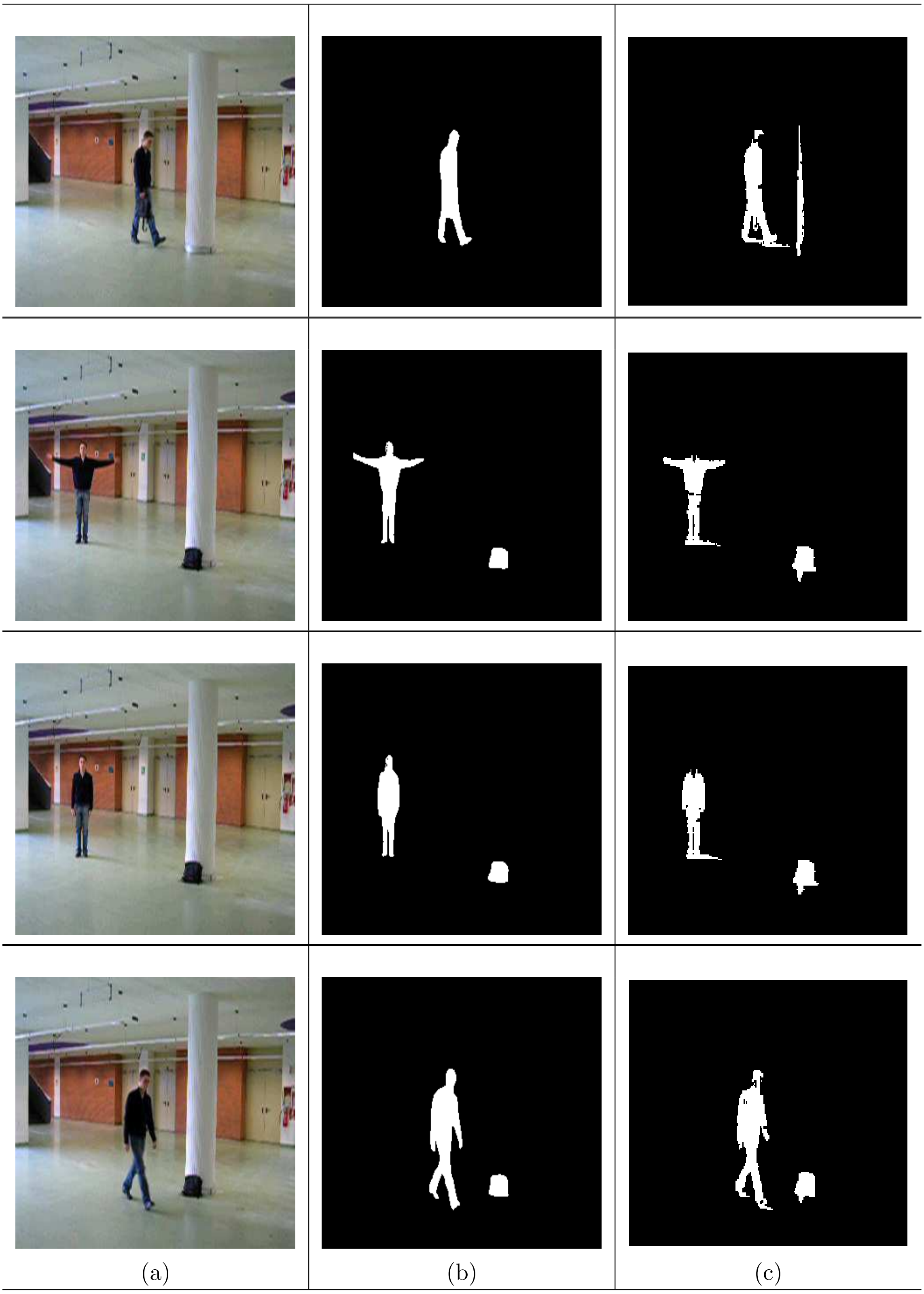

Figure 2.12: (a) MSA image (b) ground truth (c) ICA result

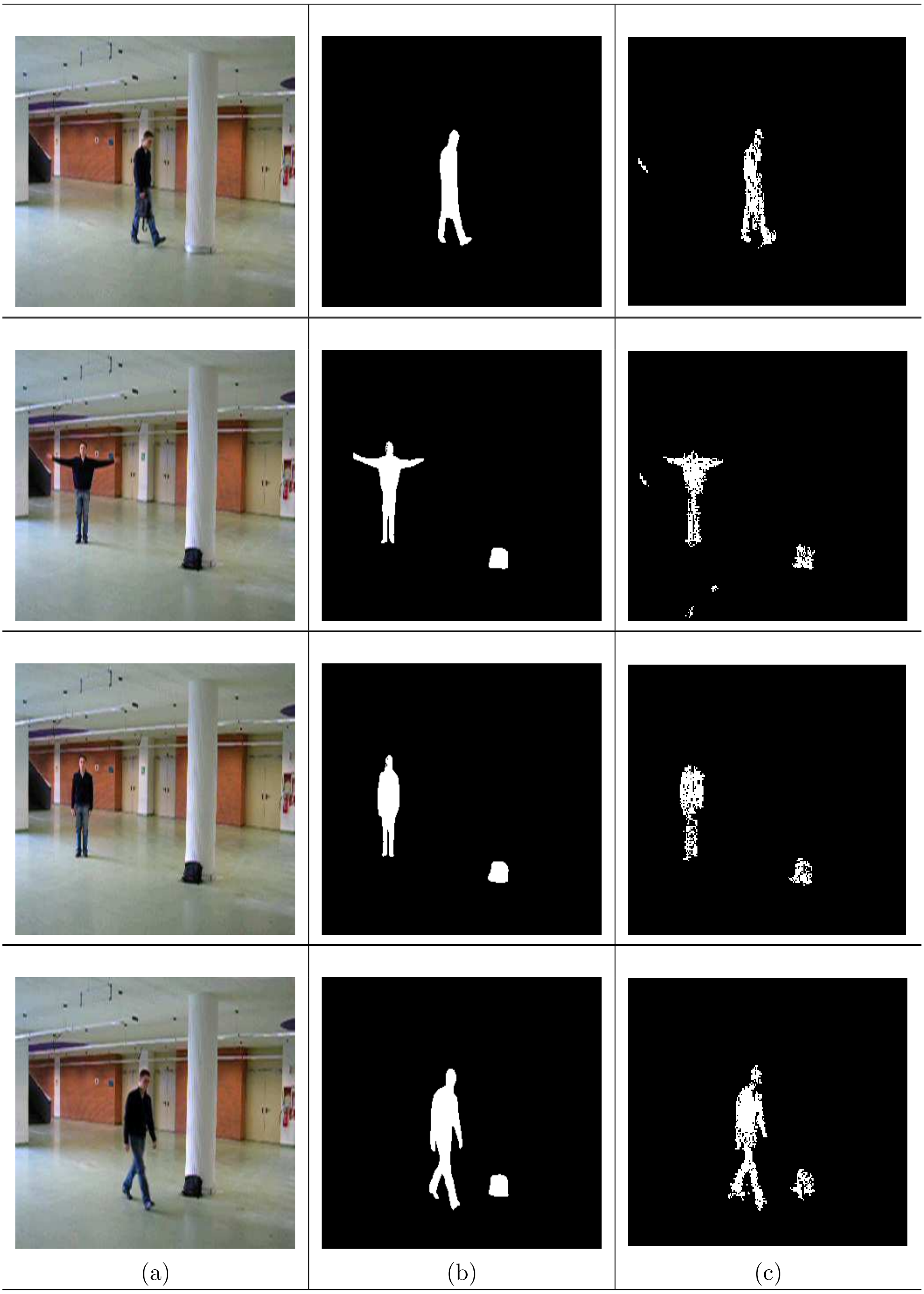

(a) (b) (c)

Figure 2.13: (a) MSA image (b) ground truth (c) SACON result

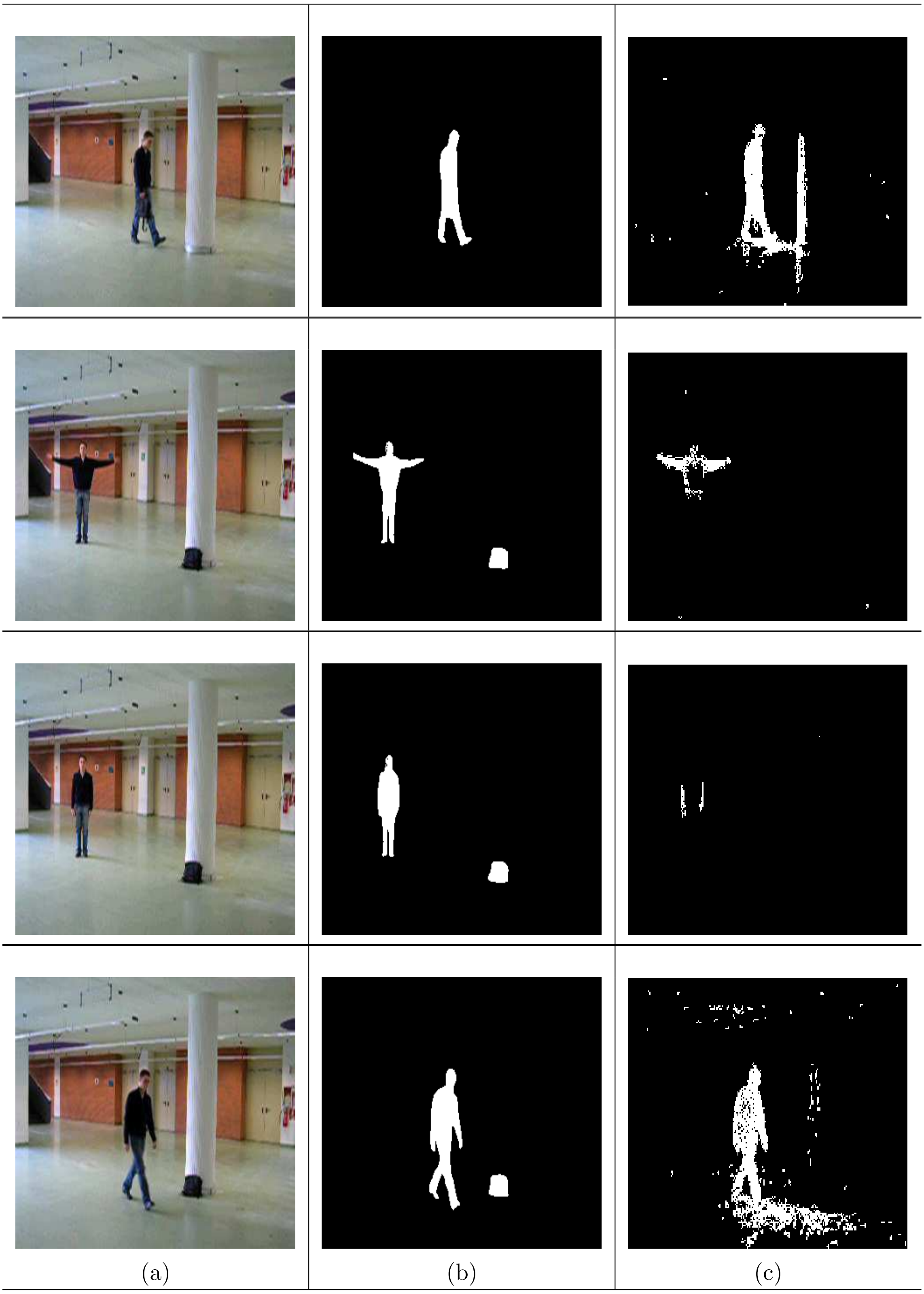

Figure 2.14: (a) MSA image (b) ground truth (c) MOG result

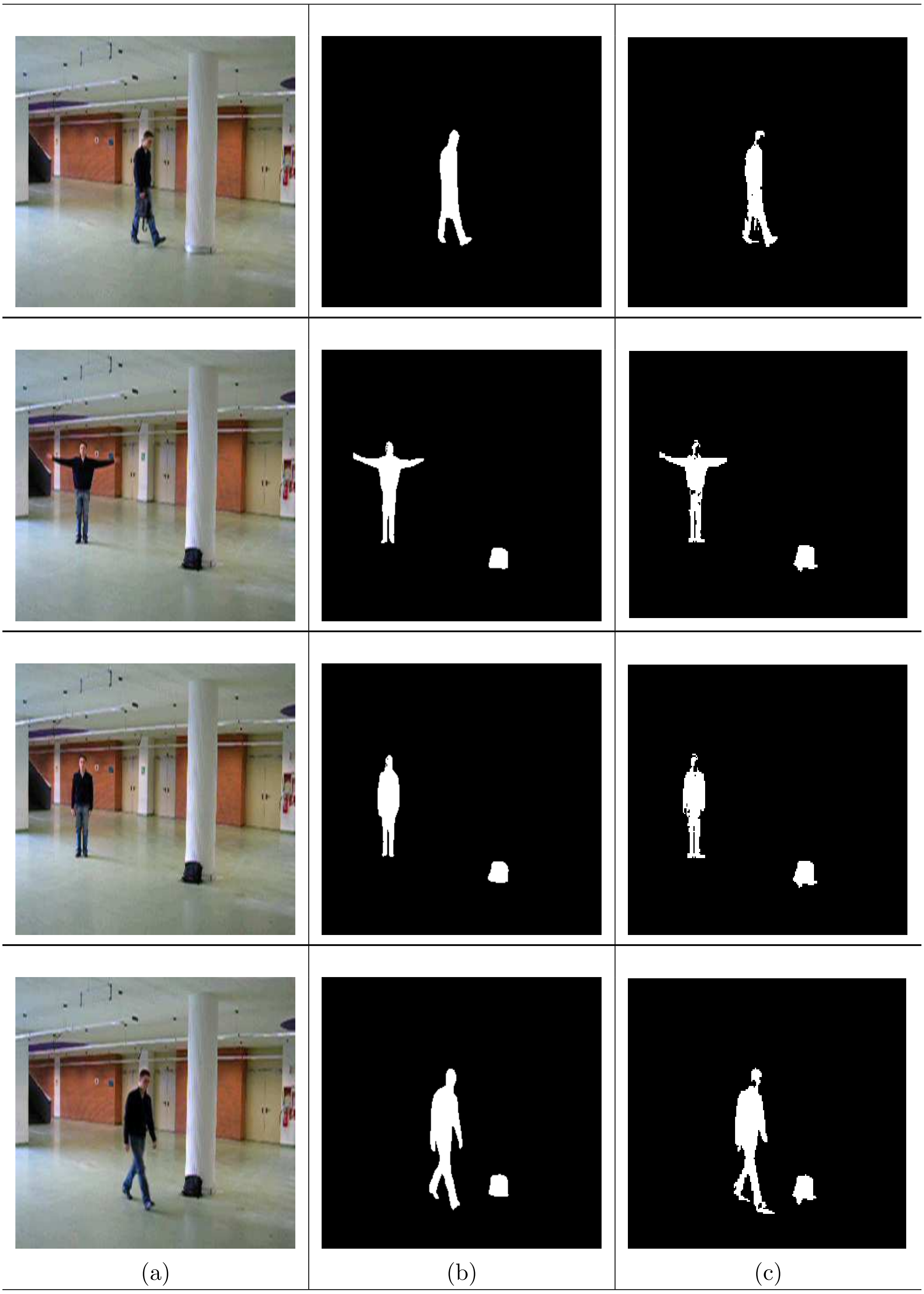

Figure 2.15: (a) MSA image (b) ground truth (c) CB result

Chapter 3

Object Classification

In visual surveillance system, motion detection is the crucial and important step that classifies the moving foreground object from the background. The segmented moving foreground object may be humans, vehicles, animals, flying birds, moving clouds, leaves of a tree, or any other noise etc. The job of a classification stage in the visual surveillance system, is to classify the moving foreground object into predefined classes such as single person, group of person, or vehicle, etc. The visual surveillance system is mostly used for humans and vehicles. Once the foreground object belongs to this class, the latter task such as personal identification, object tracking, and activity analysis of the detected foreground object can be done much more efficiently and accurately. The object classification is a standard pattern recognition problem and there are two approaches for classifying [1] moving foreground objects.

1. **Shape-based classification**: In shape-based classification, the moving foreground object region such as points, boxes, silhouettes and blobs are used for classification. Lipton et al. [4] have used image blob dispersedness and area to classify moving foreground object into human, vehicles and noise. If a target is present over a longer duration in the video, then the chances of having foreground object are high and if it is for short duration, then it is cluttered and is due to the noise in the frame. Dispersedness of an object is calculated from the given formulae.

$$Dispersedness = \frac{Perimeter^2}{Area} \tag{3.1}$$

Human body shape is complex in nature and will have more dispersedness than a vehicle. So the humans can be classified from vehicle using dispersedness and they have use Mahalanbois distance-based segmentation for foreground object classification.

2. **Motion-based classification**: The human body is non-rigid and articulated. It shows periodic motion and this property of human can be used for classification from the rest of foreground objects in the video frame. Cutler et al. [26] tracked interested object and its self-similarity is computed over time. For a periodic motion, computed self-similarity is also periodic. Time frequency analysis is done to detect and characterize the periodic motion.

3.1 Silhouette Template Based Classification

First the object to be classified is detected and segmented from video using background subtraction technique. In silhouette template based classification foreground object distance signal is computed and its similarity with the stored templates of the foreground object is found using the minimum distance and is classified into group such as human, group of humans, vehicle, and animals. The object classification is done by a two step method as follows:

Offline step: In the offline step, various objects such as humans, group of humans, vehicles and animals distance signal is computed and stored in the template database.

Online step: The object silhouette is extracted in each frame and its distance signal is computed from it. The computed distance signal is then compared with the template distance signal stored in the database. The template is then classified to the group which gives the minimum distance with the current foreground object.

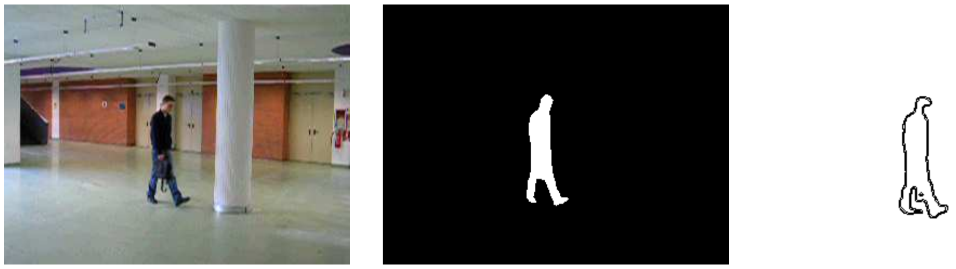

(a) (b) (c)

Figure 3.1: Illustration of object silhouette. (a) Original image (b) segmented foreground (c) object silhouette.

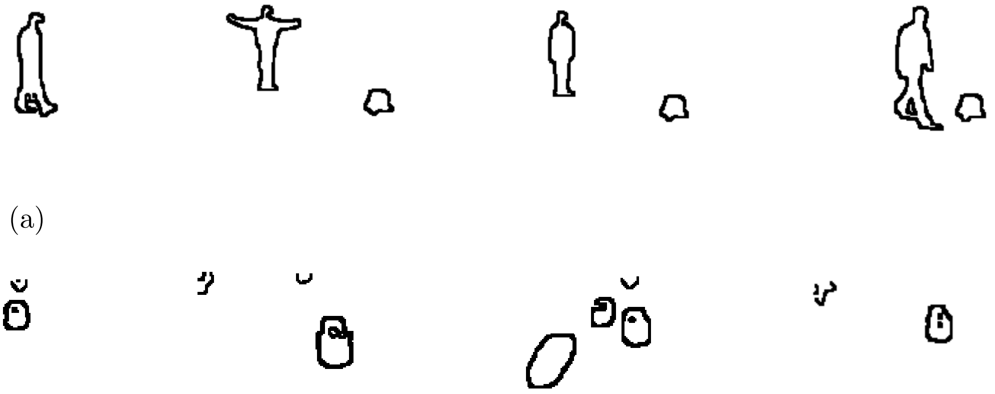

(a)

(b)

Figure 3.2: Template database of human and vehicles (a) human (b) vehicles.

3.2 Object Silhouette Extraction

First step in object classification is to extract the silhouette of the foreground object. Silhouette extraction is required both in storing the template of the database (offline) and in matching the distance signal computed from the silhouette of the foreground object with the template distance signal stored in the database. In silhouette extraction, first foreground object is segmented using background subtraction technique and then boundary following algorithm is done. Foreground object's centroid is computed (x_c, y_c), by choosing this centroid as the reference origin, the outer contour [3] is traced in counterclockwise to turn into a $1 - D$ distance signal $S = \{d\left(1\right), d\left(2\right), ..., d\left(N\right)\}$ by the given equation.

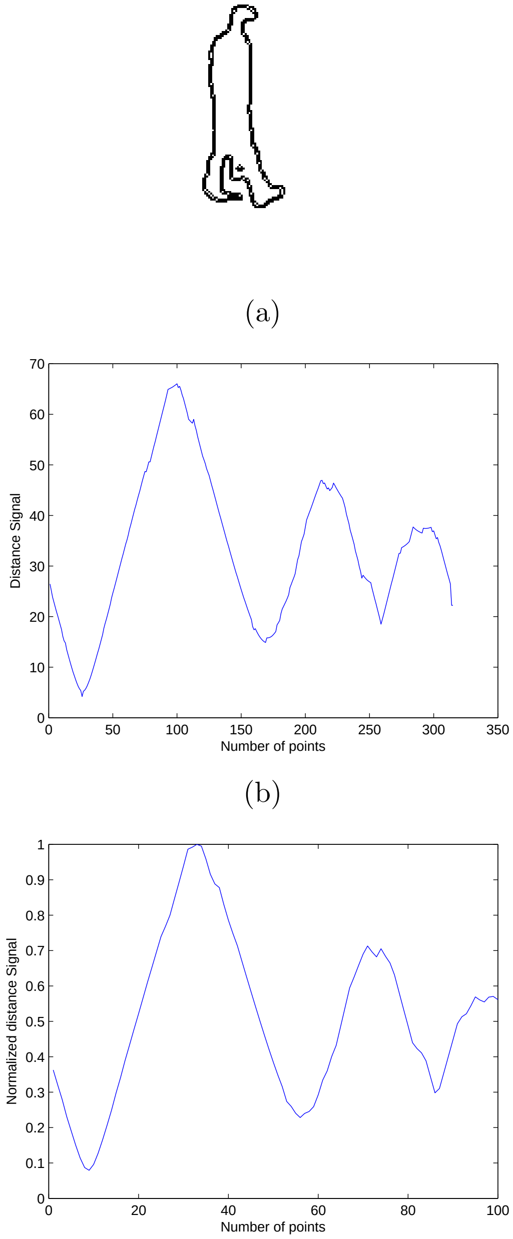

(a)

(b)

(c)

Figure 3.3: Original Image silhouette and its corresponding original distance and normalized distance signals. (a) object silhouette. (b) original distance signal. (c) normalized distance signal.

$$d\left(i\right)=\sqrt{\left(x\left(i\right)-x_c\right)^2+\left(y\left(i\right)-y_c\right)^2} \tag{3.2}$$

In different frames of a video, the size of object changes, so $1-D$ signal of same object will vary from one frame to another. To eliminate the influence of signal length and spatial scale [3], [27], $1-D$ signal length and magnitude is normalized. The 1-D signal is normalized in length by

$$\hat{S}=d\left(i*\frac{N}{C}\right),\forall i\in\left[1,...,C\right] \tag{3.3}$$

where C denotes the fixed length signal and N is the original signal length. The corresponding normalized length signal is normalized in magnitude by

$$\bar{S}\left(i\right)=\frac{\hat{S}}{\max(\hat{S})} \tag{3.4}$$

Figure 3.3 shows object silhouette and its corresponding original distance and normalized distance signal.

3.3 Target Classification

The classification metric used to classify object is similarity of object shape [27]. In order to classify the foreground object into predefined classes the minimum distance is computed between the template and the foreground object as given by

$$Dist_{AB}=\sum_{i=1}^{C}\left|S_A\left(d(i)\right)-S_B\left(d(i)\right)\right| \tag{3.5}$$

Chapter 4

Object Tracking

4.1 Introduction

Object tracking, consists in estimating the trajectory of moving objects in the video sequence. Automatic detection and tracking of moving object is very important task for human-computer interface, video communication, security and surveillance system application and so on. Here in this chapter, we use vision system to monitor activity in a place over an extended period of time. It provides a robust mechanism to find out the suspicious activities in and around the site and is very beneficial for the defense people in detecting intruders. Video surveillance can be used in monitoring the safe custody of crucial data, arms and ammunition in defense establishments. It can provide security to key installations and monuments.

It uses infrared sensors [28] to locate and track the direction of the moving object and sends out a trigger signal to video cameras for tracking. Video cameras are not always taking the video image of the site, it starts acquisition image only when it gets triggered signal from the infrared sensor. In this way this system uses less data for storing the video imagery. Infrared sensors are connected to sensor node and it is further connected to gateway as shown in Fig. 4.1. Inter-connection can be wired or wireless connection. Video surveillance cameras are connected to the gateway. The gateway is used as communication and information processing unit to process the information obtained from the infrared sensors and video cameras. Gateway is

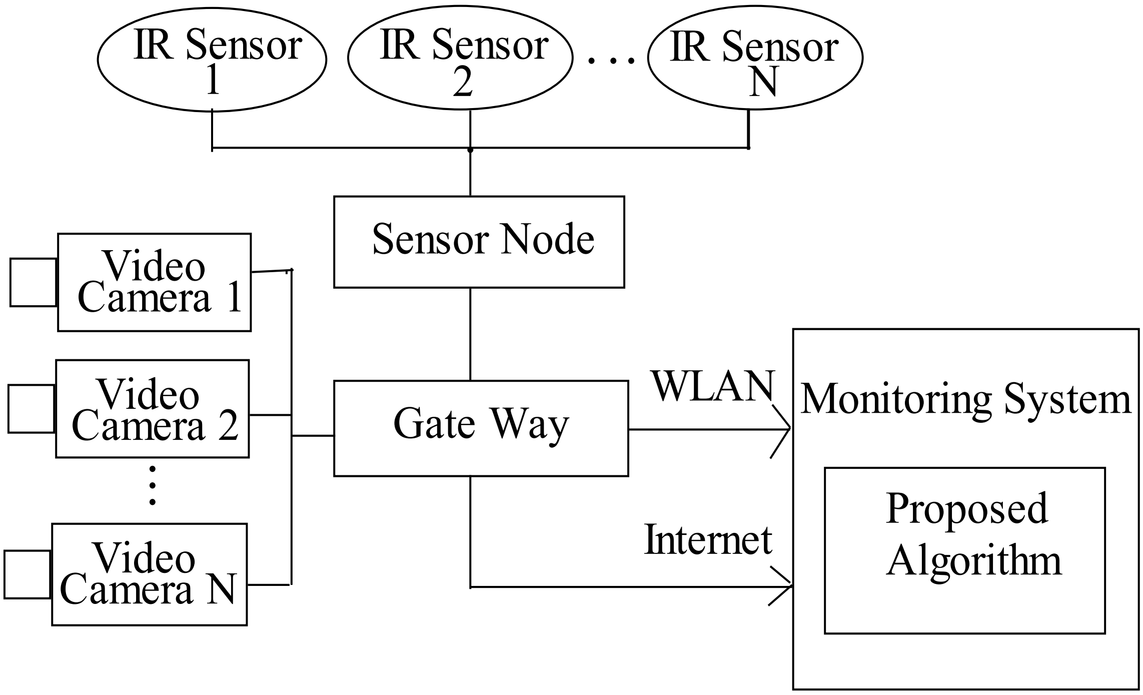

Figure 4.1: Video surveillance cameras, infrared sensor, sensor node and gateway in sensor network for intelligent tracking

a medium to communicate the video cameras and infrared sensors with the central database system, using Internet and WLAN (Wireless Local Area Network).

Every object tracking systems starts with detecting moving object in video streams. Motion segmentation not only helps in segmenting moving region from the rest of image, detecting moving objects is used for recognition, classification and activity analysis, making these latter steps more efficient. The detection of motion in many tracking systems relies on the techniques of frame differencing and background subtraction. Frame differencing is a pixel-wise differencing between two or three consecutive frames in an image sequence to detect regions corresponding to moving object such as human and vehicles. On the other hand, background subtraction detects moving regions in an image by taking the difference between the current image and the reference background image captured from a static background during a period of time.

The major problems encountered in the object tracking [29] are changes in illumination, complex object shape being tracked and occlusion in case of tracking multiple people. Some of the difficulties in tracking moving objects can be summarized as follows.

- Loss of information in projecting the 3-D image to 2-D plane,
- Noise in image video resulting in loss of information,
- Difficulty in finding the exact position of moving object in each frame,
- Partial and full object occlusions due to object or structure present in the scene,
- Complex shapes of object,
- Unobstructed view of background is not available,
- Motion in the background,
- Varying illumination condition,
- Need for real-time processing.

In object detection methodology, many researchers have developed their methods. Changes in scene lightning can cause problem for object detection. Stauffer and Grimson [11] have modeled each pixel as a mixture of Gaussians and uses an on-line approximations to update the model. This can deal with lightning changes, motions in the background, and from the long term scene changes. Maddalena and Petrosino [9] have proposed SOBS based on self organization through artificial neural networks that can handle background clutter, gradual illumination variations and camouflage, has no bootstrapping limitations, overcomes the problem of shadows cast by moving objects, and achieves robust detection for different types of videos taken from still cameras. Toyoma et al. [8] have discussed the problems of changing illumination, background clutter, camouflage and shadows, using the proposed three-component system for background maintenance: the pixel level component, the region-level component and the frame-level component.

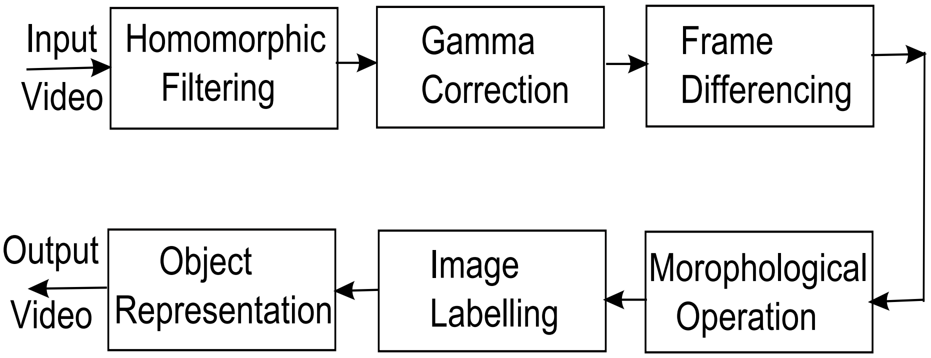

Figure 4.2: Steps in object tracking under varying illumination condition

4.2 Object Tracking under Varying Illumination Condition

In this section, a robust object tracking [30] algorithm is proposed to overcome the problem of illumination variation. It is proposed to detect and track a moving object using frame differencing. Frame differencing method is one of the simplest methods to detect and track objects for real time processing. Object detection and tracking in each frame of the video is performed by a six stage process shown in Fig.4.2.

The various sub-processes are described below.

4.2.1 Homomorphic Filtering

The input video is decomposed into frames $f(x, y, n)$ and each frame is converted into grayscale image. Here x, y are the spatial coordinates and n is the frame number that represents discrete time. A video image may be modelled as :

$$f(x, y, n) = i(x, y, n) \times r(x, y, n) \tag{4.1}$$

where $i(x, y, n)$ and $r(x, y, n)$ denote the illumination and reflectance components respectively. The nature of $i(x, y, n)$ is determined by the illumination source and $r(x, y, n)$ is determined by the characteristics of the object to be imaged. The parameters will have a range of:

$$0 < i(x, y, n) < \infty \tag{4.2}$$

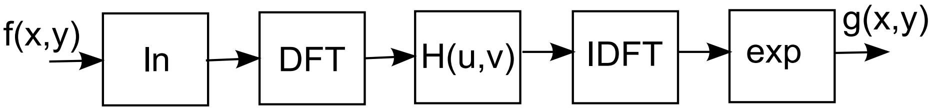

Figure 4.3: Homomorphic filtering

and

$$0 < r(x, y, n) < 1 \tag{4.3}$$

To overcome the problem of varying illumination condition, homomorphic filtering is employed here. This filtering process is depicted in Fig. 4.3. The process is performed in log domain and hence a log-transformation at the beginning and an exponentiation at the end are a must. A definite high-pass filter, characterized by its frequency-domain transfer-function $H(u, v)$,is employed to reject very low frequency components that usually represent illumination variation. To perform this frequency-domain filtering, signal is transformed to frequency-domain. Hence the DFT and inverse-DFT processes are employed as shown in the figure.

The illumination component of an image has slow spatial variations,while the reflectance component tends to vary rapidly. The problem with low cost surveillance camera is that their video imagery gets affected by the changing illumination condition. A good control over the illumination and reflectance components can be done with homomorphic filter.

Homomorphic filter function $H(u, v, n)$ is given by

$$H(u, v, n) = (\gamma_H - \gamma_L)[1 - e^{-c[D^2(u,v,n)/D_0^2]}] + \gamma_L \tag{4.4}$$

where

$$D(u, v, n) = [(u - P/2)^2 + (v - Q/2)^2]^{1/2} \tag{4.5}$$

Here u and v denote frequency-domain variables and typically $P = 2M$ and $Q = 2N$ are chosen, for frame size of $M \times N$. Constant c controls the sharpness of the slope of the function as it makes transition between γ_L and γ_H and D_0 is the cut-off frequency. $\gamma_L < 1$ and $\gamma_H > 1$ are chosen to attenuate the contribution made by the low frequencies (illumination) and amplify the contribution made by high frequencies (reflectance). As a result dynamic range is compressed and contrast is enhanced.

4.2.2 Gamma Correction

Gamma correction is a nonlinear operation used to code and decode luminance in video or still image systems. Gamma correction is defined by the following power-law expression:

$$s = cr^{\gamma} \tag{4.6}$$

where c and γ are positive constants. A gamma value $\gamma < 1$ is sometimes called an encoding gamma, and the process of encoding with this compressive power-law nonlinearity is called gamma compression. Conversely a gamma value $\gamma > 1$ is called a decoding gamma and the application of the expansive power-law nonlinearity is called gamma expansion.

4.2.3 Frame Differencing

Frame differencing is a pixel-wise difference between two consecutive frame. Each current frame is subtracted from the previous frame to detect the moving object. This is being used to detect regions corresponding to moving object such as humans and vehicles. Frame differencing is very adaptive to changing environments, but very often holes are left inside moving entities. It depends on good threshold to segment moving foreground from the background. Threshold T should be judiciously selected. If the difference is greater than the threshold T, then the value is considered to be a part of the moving object; otherwise, it is considered to be the background. Here a threshold T is chosen based on Otsu's [31] method. Otsu's method is optimum in the sense that it maximizes the between-class variance of the background and foreground.

$$D\left(x, y, n\right) = \begin{cases} 1, \text{ if } |f(x,y,n) - f(x,y,n-1)| \geq T \\ 0, \text{otherwise} \end{cases} \tag{4.7}$$

It works only when there is no camera motion, the moving object is not stationary and it is not occluded.

4.3 Object Tracking under Background Clutter

In this section, we aim to develop a robust method to handle problem related to non-stationary background such as branches and leaves of trees by decreasing spatial and intensity resolution of the video imagery. It is proposed to detect and track a moving object using frame differencing. It is one of the simplest real time processing methods to detect moving object and Fuzzy c-means (FCM) clustering is used to segment the foreground object and the background into two clusters. FCM algorithm classifies the image by grouping similar data points in the feature space into clusters.

Till now, there is no research reported on object tracking by reducing spatial and intensity resolution of image under background clutter. Here a novel and robust scheme is proposed [32] to track an object, with web camera, in presence of background clutter by reducing spatial and intensity resolution. Once three frame differencing is done, FCM algorithm is used to separate the foreground object from the background.

We have modified the work carried by Sugandi et al. [33]. Here image frames obtained from the frame differencing is not directly used for AND operation. Rather the two frames acquired, as shown in Fig.4.4, are used for filtering operation. The two frames are operated individually with morphological operation, FCM clustering and then image thresholding. Finally, the thresholded images of these two channels are ANDed and the object's position is identified. The results obtained by performing these steps are better than directly carrying out AND operation after the frame differencing and then doing filtering operation as proposed in [33].

4.3.1 Median Filtering

Smoothening of gray video imagery is done using median filter [14]. It is being done to reduce noise and increase the performance of detecting moving object. Median filter is operated with $m \times n$ pixels. Here $m \times n$ specifies the size of window. Median filter replaces the value of a pixel by the median of the intensity values in the neighborhood of that pixel in the window of $m \times n$.

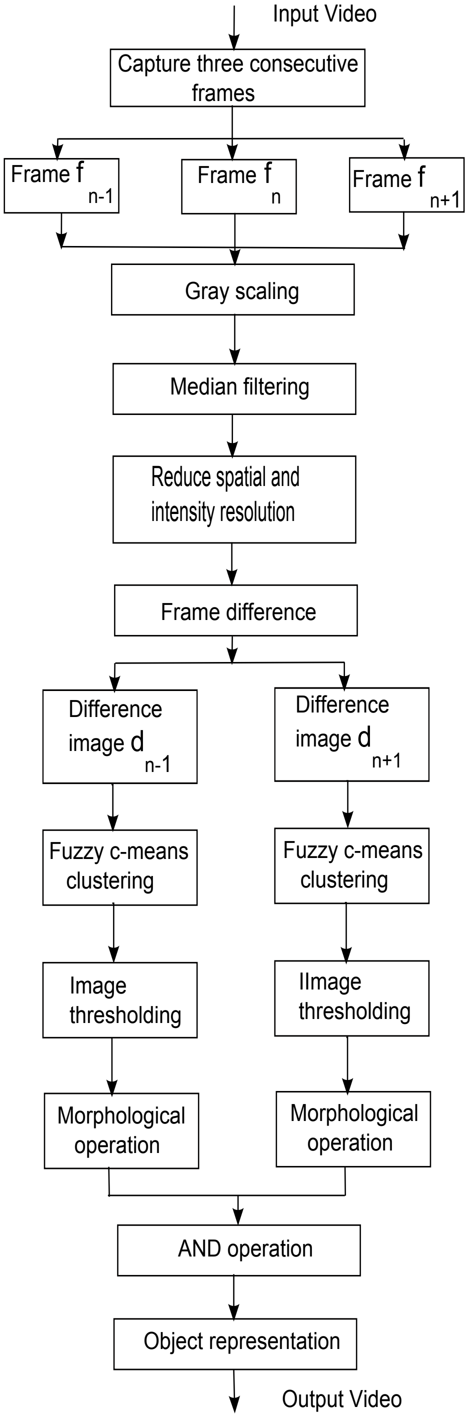

Figure 4.4: Steps in object tracking under background clutter

4.3.2 Reduction in Spatial and Intensity Resolution

Non-stationary background such as branches and leaves of trees is considered to be part of the background. But this non-stationary background is often considered as a fake motion other than the motion of the object of interest and it causes the failure

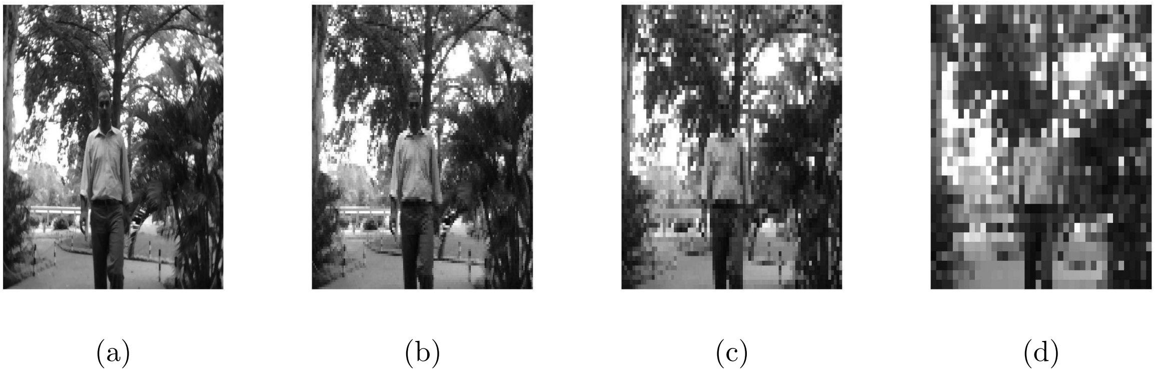

Figure 4.5: Reducing spatial resolution of an image (a) Original image (640 × 480 pixels), (b)160 × 120 pixels, (c) 80 × 60 pixels, (d) 40 × 30 pixels.

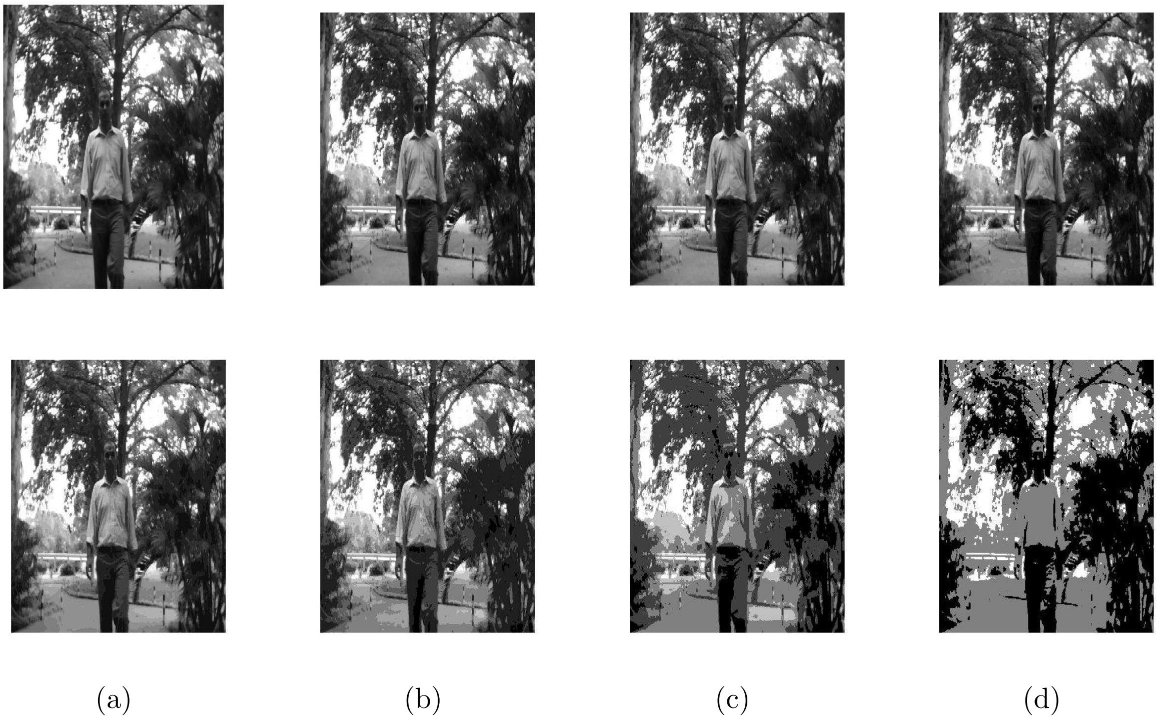

Figure 4.6: Reducing intensity resolution of an image (a) Original image (8−bit) (b) 7−bit (c) 6−bit (d) 5−bit (e) 4−bit (f) 3−bit (g) 2−bit (h) 1−bit representation

of detection of the object. To overcome the problem of non-stationary background, we reduce the spatial and intensity resolution.

(*i*) Spatial Resolution: In reducing spatial resolution [14], [33] of the image, the image size is kept constant. Here spatial resolution of image is done by averaging pixels value of its neighbors, including itself. We use a video image with resolution 640 × 480 pixels. The original image size is 640 × 480 pixels. After applying the low resolution image, the numbers of pixels is reduced to 160 × 120, 80 × 60, or 40 × 30 pixels, respectively as shown in Fig. 4.5, while the image size is still 640 × 480 pixels.

(*ii*) Intensity Resolution: In reducing intensity resolution [14], the number of bits used to represent the image is reduced from $k = 7$ to $k = 1$ as shown in Fig. 4.6 while keeping the image size constant at 640 × 480 pixels. The $256-$, $128-$, $64-$, and $32-$ level images are visually identical. In $16-$ level there is insufficient number of intensity levels for representing an digital image. Image size of 640 × 480 pixels is reduced to 40 × 30 pixels and with 64 intensity levels, the proposed algorithm sensibly tracks the moving object.

The spatial and intensity reduced resolution image is used to lessen the scattering noise and small fake motion in the background because of non-stationary background such as leaves of trees. The noise due to the non-stationary backgrounds have small motion region and it disappears in spatial and intensity reduced image.

4.3.3 Frame Differencing

Frame difference method is performed on the three successive frames, which are between frame f_n and f_{n-1} and between frame f_{n+1} and f_n. This is being used to detect moving object and to find out the regions which have changed.

$$\begin{aligned} d_{n-1} &= |f_n - f_{n-1}| \\ d_{n-1} &= |f_{n+1} - f_n| \end{aligned} \tag{4.8}$$

It works only when there is no camera motion and the moving object is not occluded or the object has not stopped motion.

4.3.4 Fuzzy C-Means Clustering

Fuzzy c-means (FCM) [34], [35] clustering is an unsupervised technique that classifies the image with N pixels $(x_1, x_2, ..., x_N)$ by grouping similar data points in the feature space into c clusters. The FCM algorithm assigns pixels to each group by using fuzzy memberships. The grouping is made by iteratively minimizing the cost function which is dependent on the distance of the pixels to the cluster centers in the feature domain. The criterion function used for fuzzy C-means clustering is given by

$$J = \sum_{j=1}^{N} \sum_{i=1}^{c} u_{ij}^{m} \left\| x_j - v_i \right\|^2 \tag{4.9}$$

where u_{ij} represent the membership of pixel x_j in the ith cluster, v_i is the ith cluster center, $\|\cdot\|$ is a norm metric, and m is constant. The parameter m controls the fuzziness of the resulting position. The membership function and cluster centers are updated by 4.10 and 4.11.

$$u_{ij} = \frac{1}{\sum_{k=1}^{c} \frac{\|x_j - v_i\|}{\|x_j - v_k\|}^{\frac{2}{m-1}}} \tag{4.10}$$

and

$$v_i = \frac{\sum_{j=1}^{N} u_{ij}^{m} x_j}{\sum_{j=1}^{N} u_{ij}^{m}} \tag{4.11}$$

FCM starts with an initial guess for the cluster centers and converges to solution of cluster center v_i .

4.3.5 Image Thresholding

The result obtained from the FCM algorithm is used for thresholding, foreground object from the background. Thresholding [14], [31] is an important technique for image segmentation based on the assumption that the objects can be distinguished and extracted from the background. Once image thresholding is done then labeling is done to label moving object emerging in the background. The connected component labeling groups the pixels into components based on pixel connectivity. In this labeling connected component is done through four neighbors.

4.3.6 AND Operation

$$m_n = d_{n-1} \cap d_{n+1} \tag{4.12}$$

AND operation is performed to find out the similarity between the two difference frames d_{n-1} and d_{n+1}. By this operation, the uncorrelated noise present in the two frames is removed.

4.4 Filtering

4.4.1 Morphological Operation

Morphological operations [14] apply a structuring element to an input image, creating an output image of the same size. Morphological operation is performed to fill small gaps inside the moving object and to reduce the noise remained in the moving objects. The morphological operators implemented are dilation followed by erosion. In dilation, each background pixel that is touching an object pixel is changed into an object pixel. Dilation adds pixels to the boundary of the object and closes isolated background pixel. Dilation of set A by structuring element B [14] is defined as :

$$A \oplus B = \bigcup_{b \in B} (A)_b \tag{4.13}$$

In erosion, each object pixel that is touching a background pixel is changed into a background pixel. Erosion removes isolated foreground pixels. Erosion of set A by structuring element B [14] is defined as:

$$A \ominus B = \bigcap_{b \in B} (A)_{-b} \tag{4.14}$$

The number of pixels added or removed from the objects in an image depends on the size and shape of the structuring element used to process the image. Morphological operation eliminates background noise and fills small gaps inside an object. This property makes it well suited to our objective since we are interested in generating masks which preserve the object boundary. There is no fixed limit on the number of times dilation and erosion is performed. In the proposed algorithm dilation and erosion is used iteratively till the foreground object is completely segmented from the background.

4.4.2 Image Labeling

After foreground region detection, a binary connected component analysis is applied to the foreground pixels to assign a unique label to each foreground object. Connected component labeling [14] is performed to label each moving object emerging in the background. The connected component labeling groups the pixels into components based on pixel connectivity. Connected component labeling is done by comparing the pixel with the pixel in four neighbors. If the pixel has at least one neighbor with the same label, this pixel is labeled as same as neighbors label.

4.5 Object Representation

Once morphological operations are over, the detected foreground object is fully visible from the background and there is less chance of misdetection of object. The segmented object is represented through centroid and rectangular shape to envelope the object. Following formulae are used to determine a centroid

$$C_x(n) = l(n)/2 \tag{4.15}$$

$$C_y(n) = b(n)/2 \tag{4.16}$$

where $l(n)$ and $b(n)$ are derived as follows:

$$l(n) = x(n)_{max} - x(n)_{min} \tag{4.17}$$

$$b(n) = y(n)_{max} - y(n)_{min} \tag{4.18}$$

Here $l(n)$ and $b(n)$ are length and breadth of the rectangular region that describes the detected foreground and $x(n)_{max}$,$x(n)_{min}$, $y(n)_{max}$, $x(n)_{min}$ are the maximum and minimum spatial coordinates of the detected foreground region.

4.6 Object Tracking using Correlation Metrics

4.6.1 Correlation metrics

Let us consider a template w and a image f, over which search for an object template needs to be carried out is an graylevel image. The position of the object can be detected by finding out the correlation of template w with every template size selection in the image f. The template w is of size $K \times L$ and image f is of size $M \times N$.

The standard $2-D$ correlation metric is given by:

$$c(m,n) = \sum_{i=0}^{K-1} \sum_{j=0}^{L-1} f(m+i, n+j) w(i,j) \tag{4.19}$$

where $c(m,n)$ is the element of the correlation matrix at row $m = 0,1,2,...,M-K+1$ and column $n = 0,1,2,...,N-L+1$.

The standard correlation in frequency domain is given as:

$$c = real(ifft(F. * W^*)) \tag{4.20}$$

where F and W are the 2-D discrete Fourier Transforms(DFT) of f and w, respectively. Before computing the DFT, f and w must be properly padded [14], [36] to avoid wraparound error. The minimum size of the zero-padded images should be $P \times Q$, where $P \geq M+K-1$ and $P \geq N+L-1$.

The correlation of the template with the image, gives a maximum value at (m_*, n_*), which is the top-left corner of the template's best match with the image. This correlation metric performance is effected in the varying illumination condition and the values of the correlation metrics are not in the range of $[-1.01.0]$.

However, normalize correlation [36] is less effected by the varying illumination condition and its values are normalized by the square-roots of the energies of the image and template. Its values are in the range of $[-1.01.0]$. Normalize correlation is given by:

$$c(m,n) = \frac{\sum_{i=0}^{K-1}\sum_{j=0}^{L-1} f(m+i,n+j)w(i,j)}{\sqrt{\sum_{i=0}^{K-1}\sum_{j=0}^{L-1} f(m+i,n+j)^2}\sqrt{\sum_{i=0}^{K-1}\sum_{j=0}^{L-1} w(i,j)^2}} \tag{4.21}$$

NC does not exist in the frequency domain.

Normalized correlation coefficient [14] is more robust to varying illumination condition and its values are in the range of $[-1.0, 1.0]$.

$$c(m,n) = \frac{\sum_{i=0}^{K-1}\sum_{j=0}^{L-1}[f(m+i,n+j)-\mu_f][w(i,j)-\mu_w]}{\sqrt{\sum_{i=0}^{K-1}\sum_{j=0}^{L-1}[f(m+i,n+j)-\mu_s]^2}\sqrt{\sum_{i=0}^{K-1}\sum_{j=0}^{L-1}[w(i,j)-\mu_w]^2}} \tag{4.22}$$

where μ_f and μ_w are the mean value of the image and the template respectively. Normalized correlation coefficient in the frequency domain is given by

$$c = real(ifft((S./\left\|S\right\|) \cdot *((W./\left\|T\right\|)))) \tag{4.23}$$

where $\|\cdot\|$ is the magnitude of the complex DFT of S and W.

4.6.2 Template Updating

In a video at every time instant t, the shape, size, orientation, etc of the object keeps on changing. So a constant template over a time will not work and the template needs to be updated at every time instant t. Let $b(t)$ be the best match produced from the correlation of template w and the image f and let $w(t)$ and $w(t+1)$ be the current and updated template. The $c_{\max}$ is the maximum peak value in the correlation metric. τ_w is the threshold whose value lies between $0 < \tau_w < 1$. Some of the template updating method [36] are discussed as follows:

Simple template updating method

$$w(t+1) = \begin{cases} b(t), \text{ if } c_{\max} > \tau_w \\ w(t), \text{otherwise} \end{cases} \tag{4.24}$$

α-Tracker template updating method

$$w(t+1) = \begin{cases} w(t) + \alpha(b(t) - w(t)), \text{ if } c_{\max} > \tau_w \\ w(t), \text{otherwise} \end{cases} \tag{4.25}$$

IIR based template [36] updating method

$$w(t+1) = \begin{cases} (t) + (1-\beta)(w(t), \text{ if } c_{\max} > \tau_w \\ w(t), \text{otherwise} \end{cases} \tag{4.26}$$

4.7 Experimental Results

The algorithm can detect and track moving object and is tested for all kinds of varied illumination conditions taken under indoor and outdoor environments. Fig. 4.7. Shows a person moving in the corridor and is subjected to the varying illumination conditions. Using homomorphic filtering process, the change in illumination is sufficiently reduced and the proposed algorithm is able to perform detection and tracking of the person. In Fig. 4.7. centroid is plotted against the number of frames. The curve clearly shows that the algorithm is able to track the person effectively in each frame.The effectiveness of the proposed scheme is demonstrated with tracking video given in Fig. 4.8.The simulation results obtained for tracking the person under different conditions are shown in Fig. 4.8(a)-(d) respectively. The rate of miss-detection and false detection is very less even under a large change in illumination.

The algorithm for background motion can detect and track moving object and is tested for indoor and outdoor environments. Fig. 4.9 shows a person moving in the outdoor environment in presence of non-stationary background such as leaves, twig and branches of tree. Fig. 4.10 shows a person moving in the corridor. Reducing the spatial and intensity resolution of the image, background variation due to the non-stationary background and change in illumination condition is sufficiently reduced and the proposed algorithm is able to perform detection and tracking of the object. It is observed from Fig. 4.9 and Fig. 4.10 that the proposed algorithm detects and tracks object under background clutter very efficiently

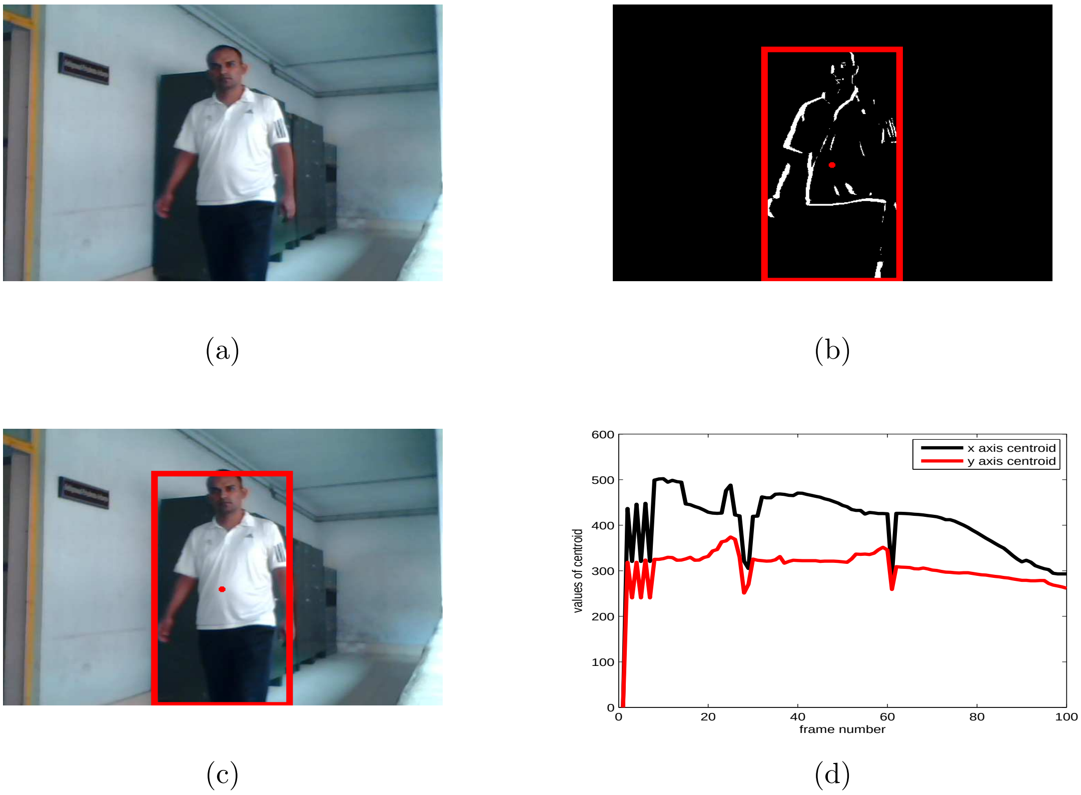

Figure 4.7: Tracking object in corridor subject to change in illumination. (a)Input Video for Object Tracking. (b)Object Tracking after Morphological Operation. (c)Tracking Object in Input Video (d)Centroid coordinates vs number of frames

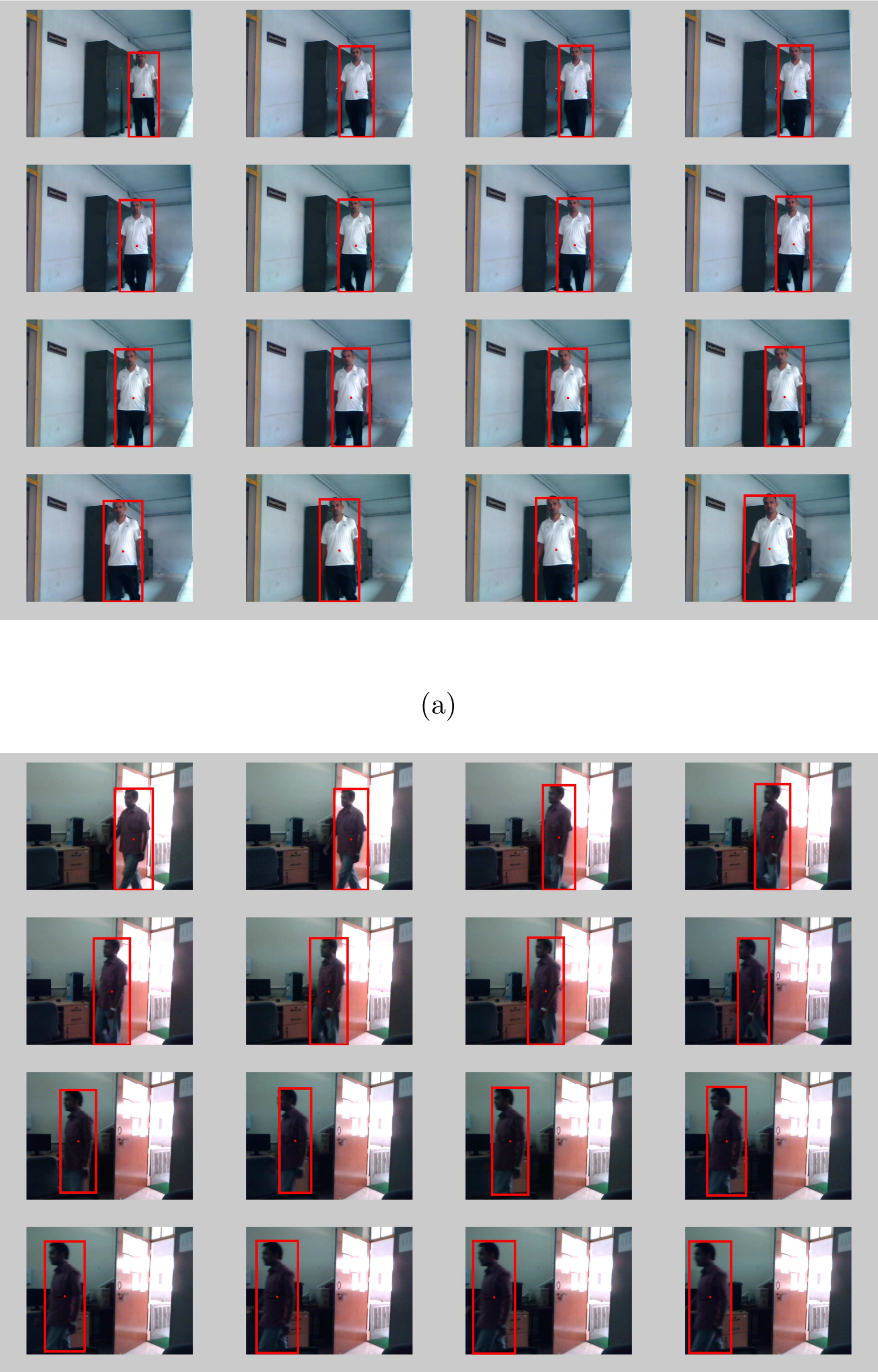

(a)

(b)

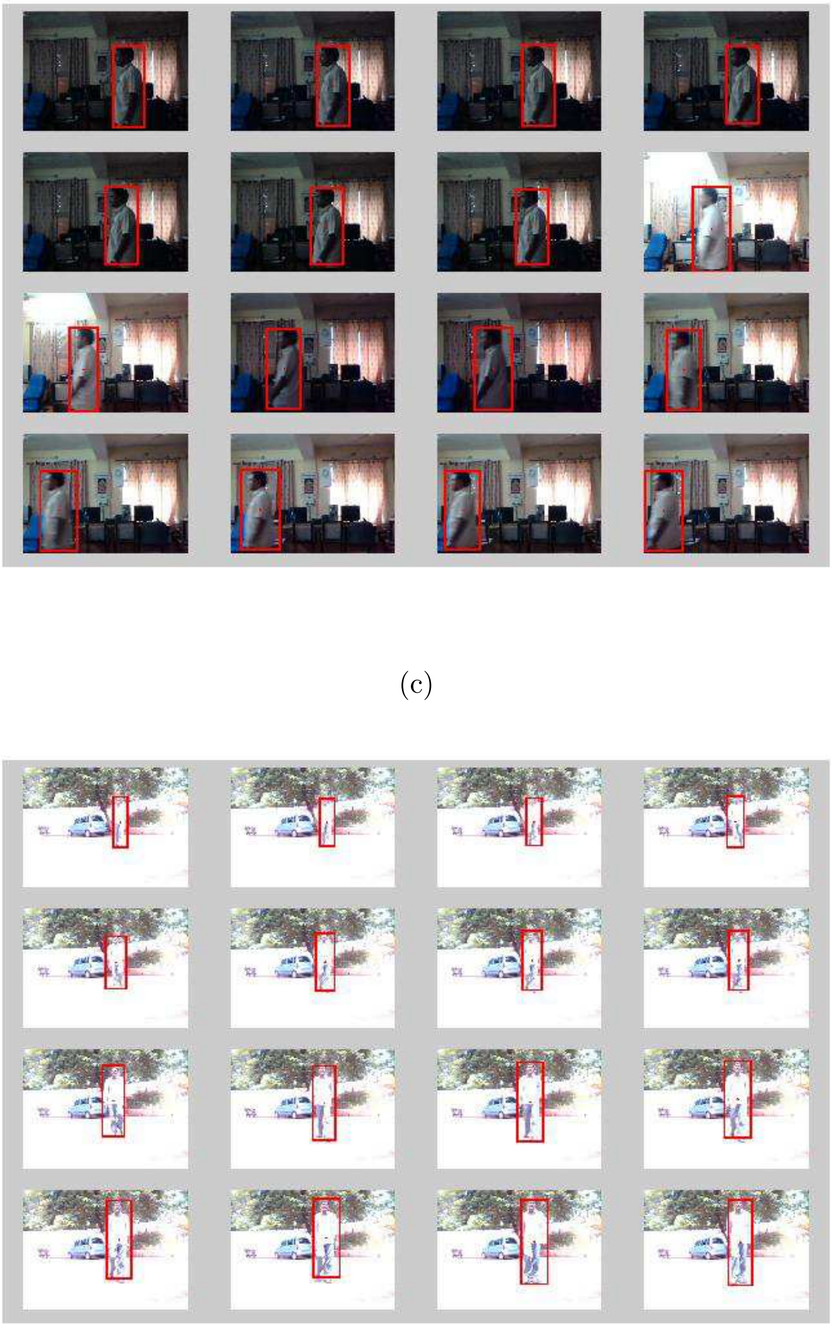

(c)

(d)

Figure 4.8: Tracking object under varying illumination conditions. (a) Person moving in the corridor. (b) Inside the laboratory. (c) Under lights on and off. (d) Outdoor environment subjected to bright light.

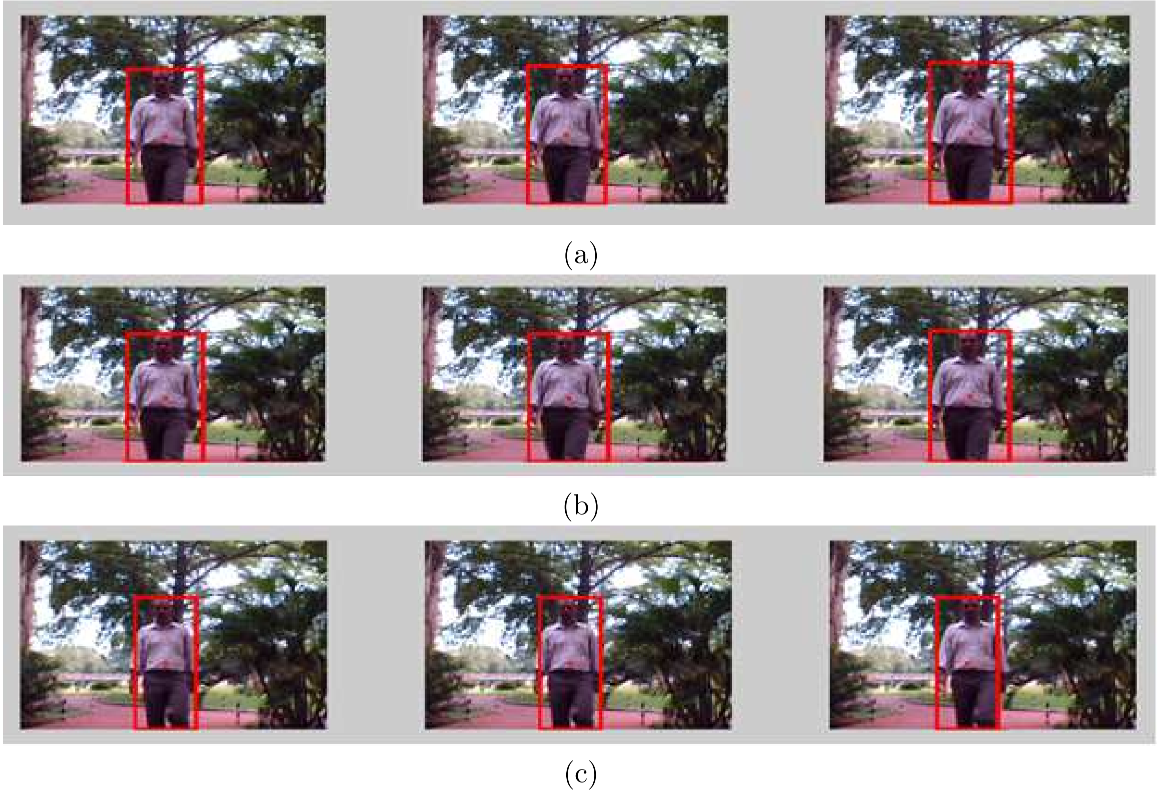

(a)

(b)

(c)

Figure 4.9: Tracking object in presence of un-stationary background such as leaves, twig and branches of tree.(a) Reduced spatial resolution to 160 × 120 pixels and each pixel is represented with 4 bit.(b) Reduced spatial resolution to 80 × 60 pixels and each pixel is represented with 4 bit.(c) Reduced spatial resolution to 40 × 30 pixels and each pixel is represented with 4 bit.

Video sequence	Total frames	Moving object	Object detected	Correct identification	Correction rate
Corridor	150	133	131	128	96.24
Indoor	50	44	41	38	92.68
lightonoff	100	84	79	76	90.47
Outdoor	150	119	117	113	94.95

Table 4.1: Performance of algorithm on different test sequence.

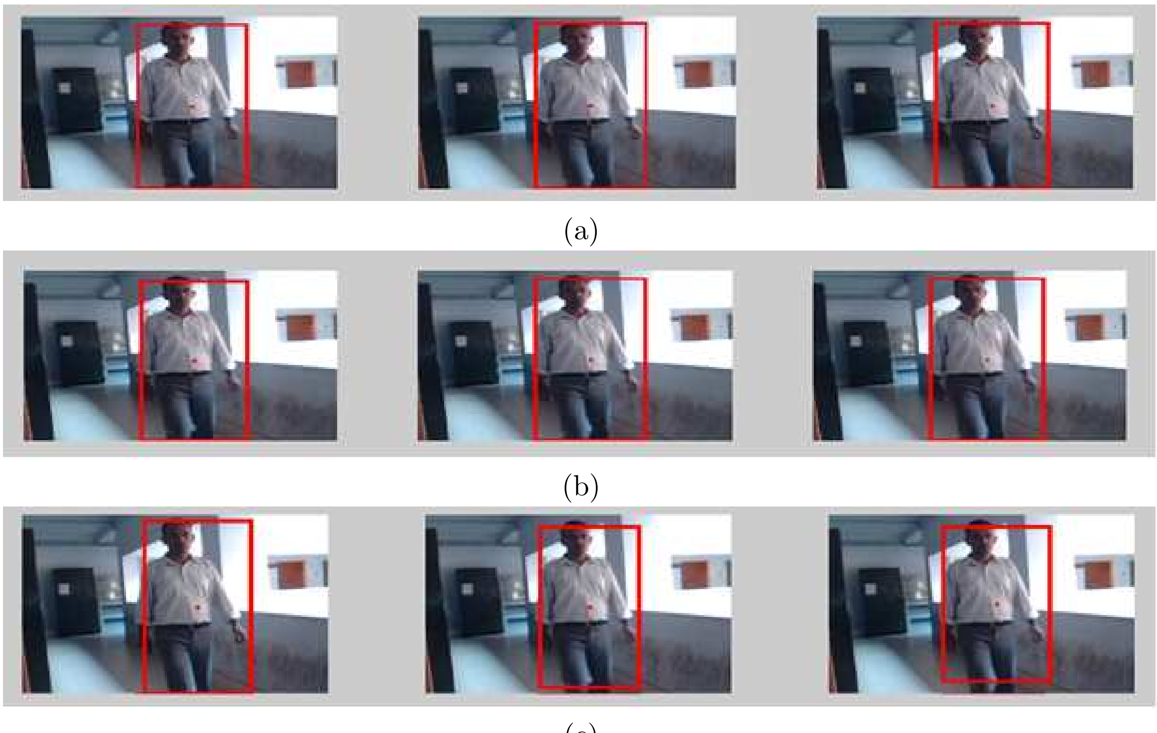

Figure 4.10: Tracking object from input video in indoor environment subjected to illumination variation.(a) Reduced spatial resolution to 160 × 120 pixels and each pixel is represented with 4 bit.(b) Reduced spatial resolution to 80 × 60 pixels and each pixel is represented with 4 bit.(c) Reduced spatial resolution to 40 × 30 pixels and each pixel is represented with 4 bit.

Spatial Resolution	Total frames	Moving object	Object detected	Correct identification	Correction rate
160×120	100	91	88	86	94.50
80 × 60	100	91	85	81	89.01
40 × 30	100	91	81	78	85.71

Table 4.2: Performance of algorithm on test sequence with background motion.

Spatial Resolution	Total frames	Moving object	Object detected	Correct identification	Correction rate
160×120	100	94	91	90	95.47
80 × 60	100	94	89	87	92.55
40 × 30	100	94	86	84	89.36

Table 4.3: Performance of algorithm on test sequence with illumination variation.

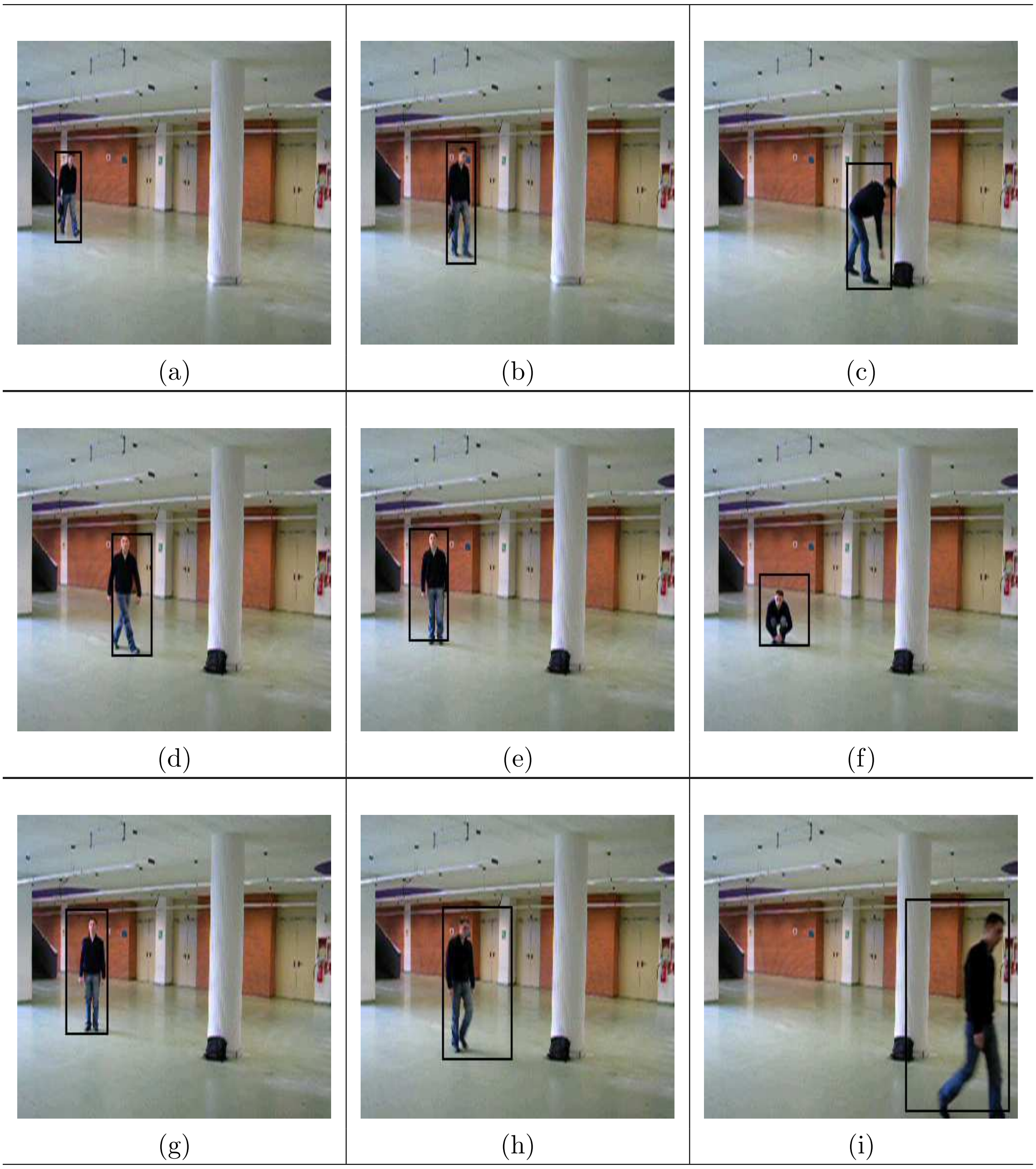

(a) (b) (c)

(d) (e) (f)

(g) (h) (i)

Figure 4.11: Tracking object using normalized correlation coefficient in MSA sequence. (a)msa 80th frame(b)msa 110th frame (c)msa 155th frame (d)msa 180th frame (e)msa 200th frame (f)msa 225th frame (g)msa 260th frame (h)msa 325th frame (i)msa 360th frame

Chapter 5

Multi-Camera Object Tracking with Non-Overlapping FOVs

Over the years, it has been seen that the busy places like the bus stand, railway station, airport, or any large public areas are under serious threat from a terrorist organization. In the past, security in public places from any untoward incident has been done by the human operator by watching multiple computer screens. However their attention level reduces over a period of time and serious incident can take place during these times. A computer vision system designed for visual surveillance can do the same job with utmost responsibility and can alert the security personnel for a deeper look into the circumstance. The job of the surveillance system is to look for abandoned object, unauthorized person, and any abnormal behavior.

A visual surveillance system designed for large public areas requires multiple camera to monitor these places. It's not possible for a single camera to cover the entire hook and nook corners of the place. In order to bring the entire region under surveillance, multiple cameras need to install, but there will be some non-overlapping regions in the camera Field of Views (FOVs) due to the finite number of camera, sensor resolution, occlusion of scene structures, economic and/or computational reasons.

Object tracking in multiple cameras with non-overlapping FoVs [37], [38] is very challenging, as problem of correspondence occurs when an object is tracked across multiple cameras. The task in hand is to determine if the object is a new object in the scene or it is a same object that is already being tracked by some other camera. Objects are often separated in time, space, as seen from different FOVs and there is a change in appearance of an object from one camera view to another. An object can take many paths across camera C_i and C_j producing different observations of the same object in two cameras. Because of the different placing of the cameras, its not possible to use space-time constraints among the exists and entrance area of the camera. Here, in this we have investigated how to track objects across multiple cameras with disjoint views using object appearances in the multi - camera FOV. Object appearance can be modeled by its color or intensity, and it is a function of scene radiance, image irradiance, exposure, and camera parameters.

This chapter gives an overall idea on how to track objects across multiple cameras with disjoint views.

5.1 Estimating Change in Appearance Between Cameras

In a single camera FOV, as an object moves there is a significant change in color of an object. For this reason, matching the appearance of an object across multi-camera is more challenging. The appearance of an object seen in multiple non-overlapping cameras [38] varies greatly due to pose, size and illumination variation. In order to match objects seen in different camera views, we have to model the changes in appearance of an object from one camera view to another by learning the changes in the color of objects, as they appear in camera FOVs from the training set. A brightness transfer function $f_{i,j}$ is estimated from the training data for camera C_i to C_j, such that the problem of correspondence is now reduced to matching transformed color histogram. $f_{i,j}$ maps an observed brightness value in camera C_i to the corresponding value in camera C_j.

Let us assume that we have a surveillance system with n non-overlapping cameras $C_1, C_2, ..., C_n$ and there are q objects $P_1, P_2, ..., P_q$ present in the scene. Each camera C_j has set of observations $O_j = \left\{O_{j,1}, O_{j,2}, ..., O_{j,m_j}\right\}$ that were generated by a moving object in the scene of the camera C_j. Each observation $O_{j,k}$ with $k = 1\ to\ m_j$ consists of two parts: object appearance $O_{j,k}(a)$ and $O_{j,k}(st)$ (position, velocity, time and etc.). Here, we have tracked objects across multiple cameras with disjoint FOVs using object appearances.

5.2 Brightness Transfer Function

Let $E_i(x, y, t)$ denotes the image irradiance [38], [39] at a spatial coordinate (x, y) at time instant t for an camera C_i. Scene radiance $R_i(x, y, t)$ is proportional to the image irradiance $E_i(x, y, t)$. The irradiance is related to radiance by a factor $P(x, y, t)$ and by exposure $e_i(x, y, t)$ as follow:

$$E_i(x, y, t) = e_i(t)P_i(x, y, t)R_i(x, y, t) \tag{5.1}$$

and scene reflectance $R_i(x, y, t)$ is a product of material $M_i(x, y, t)$ and geometry of object shape $S_i(x, y, t)$ given by:

$$R_i(x, y, t) = M_i(x, y, t)S_i(x, y, t) \tag{5.2}$$

where $P_i(x, y, t)$ is due to the optics of the system and is given by $P_i(x, y, t) = cos^4\alpha(x, y, t)/c^2$, $\alpha(x, y, t)$ is the angle subtended by the light ray from coordinate (x, y) with the optical axis and c is the focal length. $e(t)$ is the time of exposure, i.e.,$e(t) = (\pi d^2)t$, d is a lens diameter (aperture).

At a point (x, y) in the image, brightness value $B(x, y, t)$ is related to image irradiance by a nonlinear camera response function r as follow:

$$B_i(x, y, t) = r(E_i(x, y, t)) = r(M_i(x, y, t)S_i(x, y, t)P_i(x, y, t)e_i(t)) \tag{5.3}$$

If we assume two camera C_i and C_j at time instant t_i and $t_{j]}$ respectively, and at the spatial coordinate x, y material property M of an object does not change over time. So the equation can be written as:

$$M(x, y) = \frac{r_i^{-1}(B_i(x, y, t_i))}{S_i(t_i)P_i(t_i)e_i(t_i)} = \frac{r_j^{-1}(B_j(x, y, t_j))}{S_j(t_j)P_j(t_j)e_j(t_j)} \tag{5.4}$$

Brightness transfer function from the image of C_i camera at time t_i to the camera C_j at time t_j using equations 5.3 and 5.4 is given below.

$$B_j(x, y, t_j) = r_j(\frac{S_j(t_j)P_j(t_j)e_j(t_j)}{S_j(t_j)P_j(t_j)e_j(t_j)} r_j^{-1}(B_i(x, y, t_i))) = r_j(\omega(t_i, t_j))r_i^{-1}(B_i(x, y, t_i)) \tag{5.5}$$

where $\omega(t_i, t_j)$ is a function of camera parameters and the illumination and scene geometry of cameras C_i and C_j at two different time instant t_i and t_j.

$$r_j(\omega)r_i^{-1}(B_i)) = f_{ij}(B_i) \tag{5.6}$$

where f_{ij} denotes brightness transfer function (BTF) from camera C_i to camera C_j. Let H_i and H_j be the normalized cumulative histograms of object observations I_i and I_j respectively, then

$$H_i(B_i) = H_j(B_j) = H_j(f_{ij}(B_i)) \tag{5.7}$$

$$f_{ij}(B_i) = H_j^{-1}(H_i(B_i)) \tag{5.8}$$

where H^{-1} is the inverted cumulative histogram. First compute the histogram H_i and H_j from image I_i and I_j respectively. Histogram specification gives the brightness transfer function f_{ij} from camera C_i to camera C_j. The brightness transfer function is a characteristics of the camera and the exposure time and is not dependent on the scene.

A single pre-computed brightness transfer function [39] cannot be used to match objects as it varies from one frame to another due to change in illumination, scene geometry, exposure time, focal length, aperture size of each camera.

5.3 Establish BTF between cameras C_1 and C_2

Let us consider f_{12} be the BTF between the cameras C_1 and C_2 and they have object observations $O_{1,k}(a)$ and $O_{2,l}(a)$, with $k = 1, ..., M$, and $l = 1, ..., N$ represent the number of object appearance in camera C_1 and C_2 respectively. Object observation have brightness value $B_{O_{1,k}}(v)$ and $B_{O_{2,v}}(v)$, and from equation 5.8, we can say that

$$B_{O_{1,k}}(v) = f_{12}\left(B_{O_{2,v}}(v)\right) \tag{5.9}$$

where $v = 0, 1, ..., 255$ are the brightness value for an 8-bit per channel image. In order to find out the BTF f_{12} between the cameras C_1 and C_2, a total of $M + N$ histogram needs to be calculated. Let $H_{O_{1,k}}$ and $H_{O_{2,l}}$ be the normalized cumulative histograms of kth and lth object observations in cameras C_1 and C_2 respectively. There are two methods to estimate BTF f_{12} between the cameras C_1 and C_2 that is mean BTF (MBTF) $\overline{f}_{12}$ and cumulative BTF (CBTF) $\widehat{f}_{12}$.

5.3.1 Mean Brightness Transfer Function

$$\overline{f}_{12} = \sum_{k=1}^{M}\sum_{l=1}^{N} f_{O1,k}O_{2,l} \tag{5.10}$$

Mean brightness transfer function [38] (MBTF) $\overline{f}_{12}$ removes vital color information from training data set and relies heavily on different colored individuals for modeling the BTF.

5.3.2 Cumulative Brightness Transfer Function

In order to find cumulative brightness transfer function [40] (CBTF) $\widehat{f}_{12}$, a cumulative histogram $\widehat{H}_1$ is first calculated from accumulation of all brightness value observation in camera C_1. The same is done for all brightness values in camera C_2 obtaining $\widehat{H}_2$. The (CBTF) $\widehat{f}_{12}$ is computed from given formula.

$$\widehat{f}_{12}(O_{1,k}) = \widehat{H}_2^{-1}(\widehat{H}_2(O_{1,k})) \tag{5.11}$$

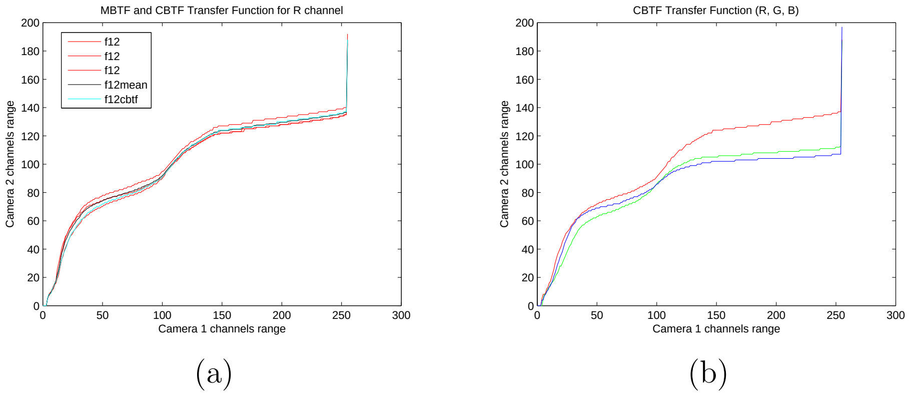

(a) (b)

Figure 5.1: Brightness transfer function from camera 1 to camera 2. (a) Mean brightness transfer function, (b) Cumulative brightness transfer function.

5.4 Multi-Camera Tracking using MBTF and CBTF

Multi-camera tracking [37] is a challenging problem as objects are often separated in time and space and object appearance changes between the cameras. In multi-camera tracking the task in hand is to establish correspondence of the object coming from different multiple cameras the one that produces the best match.

Let us consider $H_{O_{1,k_1}}, H_{O_{1,k_2}}, ..., H_{O_{1,k_{N_k}}}$, the N_k object appearances histograms of the kth person in the camera C_1. Suppose that we have P, i,e. $k \in 1, ..., P$ people moving in the camera C_1. When a kth person enters camera C_2, we have to decide, whether it is a same kth person entered or a new person has entered the camera C_2 FOV. The mean histogram of the kth person as seen in camera C_2 is given by:

$$\breve{H}_k = \bar{f}_{12}(\bar{H}_{1,k}) \tag{5.12}$$

and

$$\tilde{H}_k = \hat{f}_{12}(\bar{H}_{1,k}) \tag{5.13}$$

Let $H_{O_{2,l_1}}$ be the first observation in camera C_2. The association of the kth person is done by finding out the maximum similarity of with $H_{O_{2,l_1}}$ as given by

$$\arg\max Similarity(H_{O_{2,l_1}}, \overline{H}_{cbtf_k}) \tag{5.14}$$

$$Similarity(O_{i,k}, O_{j,l}) = 1 - D_B(O_{i,k}, O_{j,l}) \tag{5.15}$$

$$D_B(H_i, H_j) = \sqrt{1 - \sum_{v=1}^{m} \sqrt{H_i(v), H_j(v)}} \tag{5.16}$$

where $D_B(H_i, H_j)$ is the Bhattacharya distance between normalize histogram of H_i and H_j of the observations $O_{i,k}$ and $O_{j,l}$. The total number of histogram bins m, for 8-bit image the maximum bin is 256.

5.5 Experimental Results

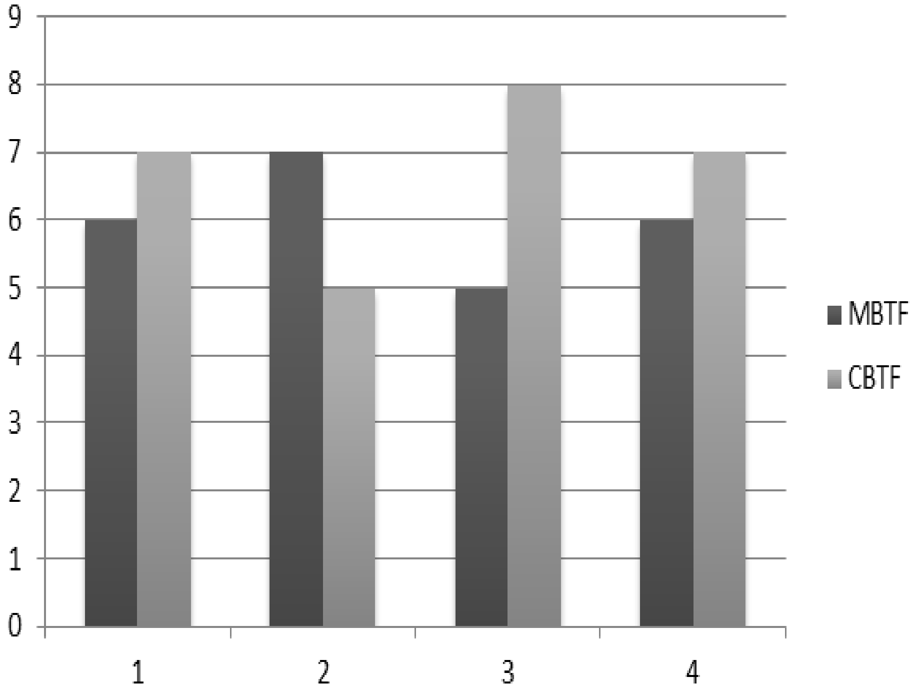

Figure 5.2: Results of matching comparison from camera 1 to camara 2 with MBTF and CBTF

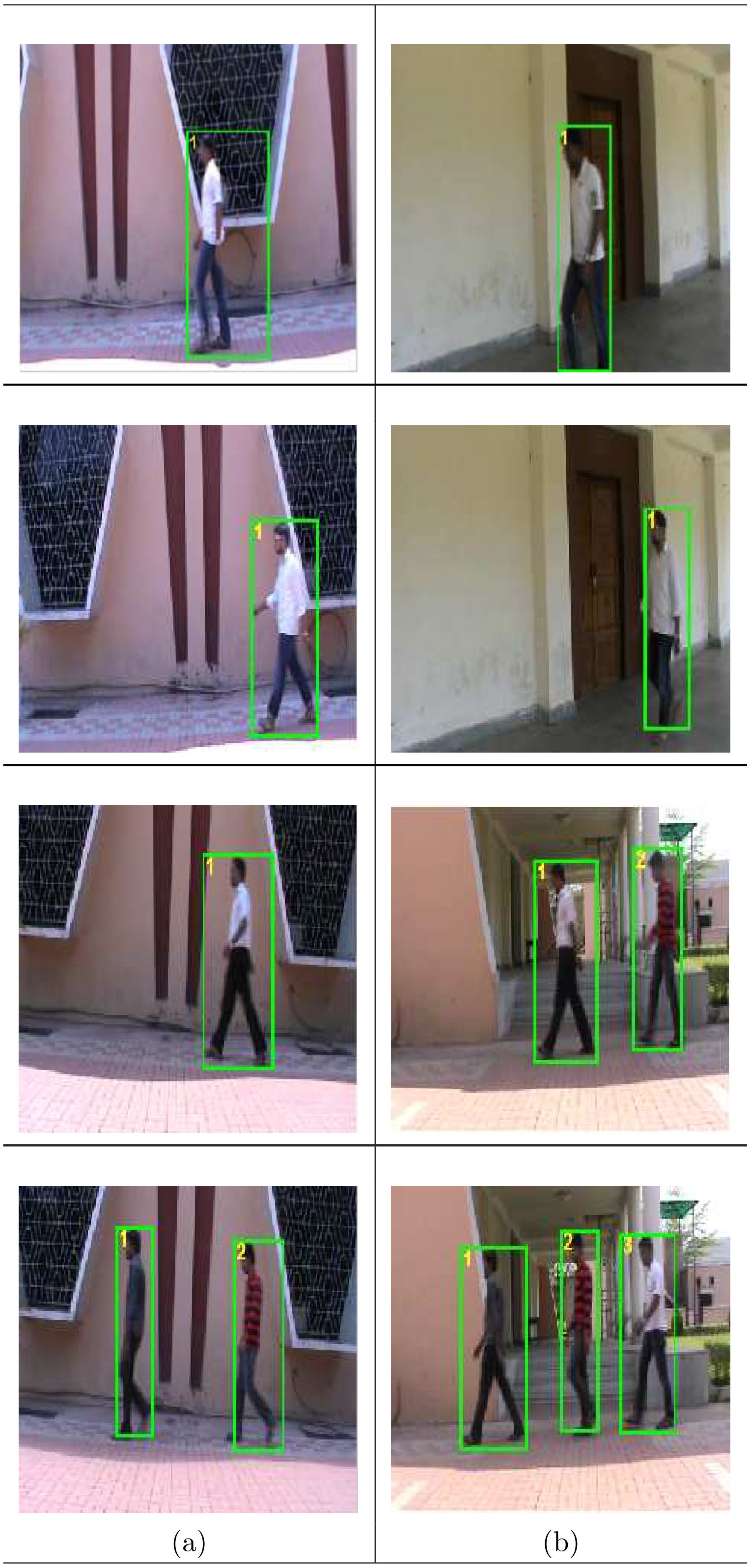

(a) (b)

Figure 5.3: Tracking across camera 1 and camera 2 with non-overlapping FOVs (a) Camera 1 image (b) Camera 2 image.

Chapter 6

Conclusions and Future Work

Here in this thesis, we have presented the methods for visual surveillance and have carried out the work on motion detection, object classification, single camera object tracking and multiple camera object tracking in non-overlapping FoVs. In motion detection, a study on different recent background subtraction available in the literature have been studied and their performance tests on the different video test sequence. It should be noted that robust motion detection is a critical task and its performance is affected by the presence of varying illumination, background motion, camouflage, shadow, and etc.

In object classification, object has been classified computing the distance signal from silhouette and then finding out the Euclidean distance between the object and template stored.

In single camera object tracking, we have proposed two methods to overcome the problem of varying illumination condition and background clutter. Target tracking of interested object is being done using the normalized cross correlation (NCC) and updating the template.

In multiple camera object tracking, matching of object is being done from one camera to another by using the appearance of an object and then computing the Bhattacharya distance between the two.

Future work includes the personal identification using gait and face recognition. One of the important steps in visual surveillance system is activity recognition, such that the behavior of the suspected person can be done is our future task. In multiple camera object tracking, the re-identification of an object from one camera to another is an issue and using the appearance feature of the object cannot improve the result. As appearance depends on size and color of an object and these two parameters varies greatly in frames of a single camera and the variation is more in multiple camera. The results can be further improved, if in addition to appearance, the height of an object is also taken into account.

1. **Deepak Kumar Panda**, and Sukadev Meher. Robust Object Tracking Under Background Clutter. In *Proceedings of International Conference on Image Information Processing*, Nov. 2011 JUIT Shimla, India.

2. **Deepak Kumar Panda**, and Sukadev Meher. Robust Object Tracking Under Varying Illumination Conditions. In *Proceedings of IEEE India Conference INDICON*, Dec 2011. BITS Pilani Hyderabad Campus, India.

Bibliography

[1] Weiming Hu, Tieniu Tan, Liang Wang, and S. Maybank. A Survey on Visual Surveillance of Object Motion and Behaviors. *IEEE Transactions on Systems, Man and Cybernetics, Part C (Applications and Reviews)*, 34(3):334–352, August 2004.

[2] N. Buch, S. A. Velastin, and J. Orwell. A review of computer vision techniques for the analysis of urban traffic. *IEEE Transactions on Intelligent Transportation Systems*, 12(3):920–939, 2011.

[3] L. Wang, T. Tan, H. Ning, and W. Hu. Silhouette analysis-based gait recognition for human identification. *TPAMI*, 25(12):1505–1518, 2003.

[4] Alan J. Lipton, Hironobu Fujiyoshi, and Raju S. Patil. Moving target classification and tracking from real-time video. In *Proceedings of the 4th IEEE Workshop on Applications of Computer Vision (WACV'98)*, WACV '98, pages 8–. IEEE Computer Society, 1998.

[5] J. L. Barron, D. J. Fleet, and S. S. Beauchemin. Performance of optical flow techniques. *INTERNATIONAL JOURNAL OF COMPUTER VISION*, 12:43–77, 1994.

[6] O. Barnich and M. Van Droogenbroeck. ViBe: A Universal Background Subtraction Algorithm for Video Sequences. *IEEE Transactions on Image Processing*, 20(6):1709–1724, June 2011.

[7] Ahmed Elgammal, David Harwood, and Larry Davis. Non-parametric model for background subtraction. In *FRAME-RATE WORKSHOP, IEEE*, pages 751–767, 2000.

[8] K Toyama, J Krumm, B Brumitt, and B Meyers. Wallflower: principles and practice of background maintenance. *Proceedings of the Seventh IEEE International Conference on Computer Vision*, 1(c):255–261, 1999.

[9] L. Maddalena and A. Petrosino. A Self-Organizing Approach to Background Subtraction for Visual Surveillance Applications. *IEEE Transactions on Image Processing*, 17(7):1168–1177, 2008.

[10] Ismail Haritaoglu, David Harwood, and Larry S. Davis. W4: Real-time surveillance of people and their activities. *IEEE Transactions on Pattern Analysis and Machine Intelligence*, 22:809–830, 2000.

[11] Chris Stauffer, W. Eric, and W. Eric L. Grimson. Learning patterns of activity using real-time tracking. *IEEE Transactions on Pattern Analysis and Machine Intelligence*, 22:747–757, 2000.

[12] Antoine Manzanera and Julien C. Richefeu. A new motion detection algorithm based on [Sigma]-[Delta] background estimation. *Pattern Recognition Letters*, 28(3):320–328, February 2007.

[13] Shih-Chia Huang. An advanced motion detection algorithm with video quality analysis for video surveillance systems. *IEEE Transactions on Circuits and Systems for Video Technology*, 21(1):1 – 14, January 2011.

[14] Rafael C. Gonzalez and Richard E. Woods. *Digital Image Processing (3rd Edition)*. Prentice Hall, 3 edition, August 2007.

[15] Thanarat Horprasert, David Harwood, and Larry S. Davis. A robust background subtraction and shadow detection. In *In Proceedings of the Asian Conference on Computer Vision*, 2000.

[16] Du-Ming Tsai and Wei-Yao Chiu. Motion detection using fourier image reconstruction. *Pattern Recogn. Lett.*, 29(16):2145–2155, December 2008.

[17] Du-Ming Tsai and Shia-Chih Lai. Independent component analysis-based background subtraction for indoor surveillance. *Trans. Img. Proc.*, 18(1), January 2009.

[18] Y. Shi and R. Eberhart. A modified particle swarm optimizer. *Evolutionary Computation Proceedings, 1998. IEEE World Congress on Computational Intelligence., The 1998 IEEE International Conference on*, pages 69–73, May 1998.

[19] Hanzi Wang and David Suter. A consensus-based method for tracking: Modelling background scenario and foreground appearance. *Pattern Recogn.*, 40(3), March 2007.

[20] S. McKenna. Tracking Groups of People. *Computer Vision and Image Understanding*, 80(1):42–56, October 2000.

[21] A Mittal and N Paragios. Motion-based background subtraction using adaptive kernel density estimation. *Proceedings of the 2004 IEEE Computer Society Conference on Computer Vision and Pattern Recognition 2004 CVPR 2004*, 2:302–309, 2004.

[22] Weiqiang Wang, Jie Yang, and Wen Gao. Modeling Background and Segmenting Moving Objects from Compressed Video. *IEEE Transactions on Circuits and Systems for Video Technology*, 18(5):670–681, April 2008.

[23] Wallflower http://research.microsoft.com/en-us/um/people/jckrumm/wallflower/testimages.htm.

[24] Kyungnam Kim, Thanarat H. Chalidabhongse, David Harwood, and Larry Davis. Real-time foreground-background segmentation using codebook model. *Real-Time Imaging*, 11(3):172–185, June 2005.

[25] Msa test sequence http://cvprlab.uniparthenope.it.

[26] Ross Cutler and Larry Davis. Robust real-time periodic motion detection, analysis, and applications. *IEEE Transactions on Pattern Analysis and Machine Intelligence*, 22:781–796, 1999.

[27] Yigithan Dedeoglu. Moving object detection, tracking and classification for smart video surveillance. Master's thesis, Institute of Engineering and Science of Bilkent University, August, 2004.

[28] Guofang Tu, Shaoshuai Gao, and Can Zhang. Object tracking and qos control for wireless sensor networks. *Chinese Journal of Electronics*, 18(4):724–728, 2009.

[29] Alper Yilmaz, Omar Javed, and Mubarak Shah. Object tracking: A survey. *ACM Comput. Surv.*, 38(4):13, December 2006.

[30] Deepak Kumar Panda and Sukadev Meher. Robust real-time object tracking under varying illumination condition. In *INDICON 2011 - Proceedings: 2011 IEEE INDICON*, pages Birla Institute of Technology and Science, Pilani; IEEE; IEEE India Council; IEEE Hyderabad Section, 2011.

[31] N. Otsu. A threshold selection method from gray-level histograms. *IEEE Transactions on Systems, Man and Cybernetics*, 9(1):62–66, January 1979.

[32] Deepak Kumar Panda and Sukadev Meher. Robust real-time object tracking under background clutter. In *ICIIP 2011 - Proceedings: 2011 International Conference on Image Information Processing*, page Jaypee University of Information Technology (JUIT), Waknaghat, Shimla, Himachal Pradesh, India, 2011.

[33] Budi Sugandi, Hyoungseop Kim, Joo Kooi Tan, and Seiji Ishikawa. Tracking of moving objects by using a low resolution image. In *Proceedings of the Second International Conference on Innovative Computing, Informatio and Control*, ICICIC '07, pages 408–, 2007.

[34] K.S. Chuang, H.L. Tzeng, S. Chen, J. Wu, and T.J. Chen. Fuzzy c means clustering with spatial information for image segmentation. *Elsevier Science journal of Computerized Medical Imaging and Graphics*, 30:9–15, 2006.

[35] Zexuan Ji, Yong Xia, Qiang Chen, Quansen Sun, Deshen Xia, and David Dagan Feng. Fuzzy c-means clustering with weighted image patch for image segmentation. *Appl. Soft Comput.*, 12(6):1659–1667, June 2012.

[36] Javed Ahmed, M. N. Jafri, Mubarak Shah, and Muhammad Akbar. Real-time edge-enhanced dynamic correlation and predictive open-loop car-following control for robust tracking. *Mach. Vision Appl.*, 19(1):1–25, January 2008.

[37] Edited by Hanna Goszczynska. *Object Tracking.* INTECH open acess, February, 2011.

[38] Omar Javed, Khurram Shafique, Zeeshan Rasheed, and Mubarak Shah. Modeling inter-camera space-time and appearance relationships for tracking across non-overlapping views. *Comput. Vis. Image Underst.*, 109(2):146–162, February 2008.

[39] M. D. Grossberg and S. K. Nayar. Determining the camera response from images: What is knowable? *IEEE Trans. on PAMI*, 25(11):1455–1467, November 2003.

[40] B. Prosser, S. Gong, and T. Xiang. Multi-camera matching using bi-directional cumulative brightness transfer functions. In *Proc. BMVC*, pages 64.1–64.10, 2008.